

Fabrication of Polymeric Membrane for Water Treatment by using Reverse Osmosis Technology



By

Inamullah khan

**School of Chemical and Materials Engineering
National University of Sciences and Technology**

2020

Fabrication of Polymeric Membrane for Water Treatment by using Reverse Osmosis Technology



Name: Inamullah khan

Reg. No.: 00000277508

**This work is submitted as a MS thesis in partial fulfillment of the
requirement for the degree of**

MS in Chemical Engineering

Supervisor Name: Dr. Tayyaba Noor

School of Chemical and Materials Engineering (SCME)

National University of Sciences and Technology (NUST)

H-12 Islamabad, Pakistan

July, 2020

Dedication

I dedicate this work to my parents, whose unwavering support and confidence in my abilities has made this work much easier

Acknowledgements

All praise belongs to Allah Almighty, the Most Benevolent, the Most Merciful, who has granted me the strength, courage and willpower to complete my work, and to overcome all the impediments that come in my way. I consider myself, highly fortunate to be able to complete this work in the time allotted to me.

My outmost gratitude to my supervisor, **Dr. Tayyaba Noor**, for her immense and unflinching support for completing my work. I am thankful to her for always believing in my abilities, and always being there for my assistance.

I owe a huge debt of gratitude to my Guidance and Examination Committee (GEC) members, **Dr. Sarrah Farrakh (Co supervisor), Dr. Arshad Hussain, Dr. Muhammad Ahsan and Dr. Erum Pervaiz**, for their advice in easing the difficulties and removing many problems in my project. I am also thankful to them for their moral as well as material assistance.

I would also like to thank the lab staff for their help in carrying out the required testing and characterization techniques. I am thankful, especially to Mr. Malik Nouman Shahzad and Mr. Zarar Saladin from SCME, and Dr. Tahir Ali from PINSTECH for their invaluable help in lab.

Finally, I am immensely gratified to my family and friends, who have been the source of endless support and encouragement for me, especially when I was in troubled waters regarding my project. They have given me much needed moral support, to complete my work.

Abstract

Water is one of the most abundant source in the world. Ground water fulfils much of our needs However, the presence of certain salts, excess minerals and other hazardous impurities may reduce the purity of the water. Salts have the most adverse effect in this regard. It is mainly present in the order of 3-4% in water, and increased amount reduces purity content of the water. Therefore it is imperative to separate salts from the water. For this purpose, it is proposed to use a polymeric membrane, which consists of TiO_2 incorporated in a Polyamide (PA-6) matrix, or a polymer blend membrane. Amine modification of the TiO_2 helps in the capture of salts like CaCl_2 , MgCl_2 . The use of Polyamide loaded with TiO_2 is helpful because of its flexible structure and fixed but tunable pores. Blend membranes work in much the same way, by including such groups in the matrix which have affinity for salts. In the present work, synthesis of a series of polymer blend membranes, consisting of a blend of polyamide (PA-6)/Formic Acid(FA) and DEMAC in an formic acid solvent system, and membranes of consist of Polyamide-6 in FA matrix, synthesized from a solution of the polymer and filler in formic Acid(FA) is carried out. These two membranes were then tested for water permeation using single and mixed water permeation testing (in water testing device which was designed), analyzed for their tensile strength using the Ultimate Tensile Testing Machine, their morphology and surface characteristics studied using SEM analysis and the presence of functional groups , salt rejection % and TiO_2 was confirmed using FT-IR ,UV and XRD spectroscopy. It was found that the amino-modified TiO_2 based PA membranes provided much better and superior single and mixed salts rejection % of 97.50% and 98.45% respectively for the membranes containing 20% polyamide (PA-6) in the formic acid, with permeability up to 38.5 ($\text{L}/\text{m}^2\text{hr}$). The membranes also exhibited uniformly pores structures, with pores observed under SEM magnifications up to 25000x. Moreover, they had a maximum tensile strength of about 20.673 MPa to 39.56MPa.

Table of contents

Dedication	i
Acknowledge	ii
Abstract	iii
List of figure	iv
List of table	v
List of Acronyms	vi
Chapter 1	1
Introduction	1
Background	1
1.1 Introduction to polymer blend membrane	5
1.1.1 Introduction to Hollow membrane	5
1.1.2 Introduction to Metal organic frame work	6
1.1.3 Use of TiO ₂ in poly amide -6 membrane	6
1.1.4 Motivation	7
1.2 Outline of thesis	9
Chapter 2	10
Literature Review	11
2.1 Application of Blend Membrane	11
2.2 Use of polymer blend membrane for water purification.	12
2.3 Use of TiO ₂ for salt separation	13
2.4 Use of TiO ₂ for water permeation	14
2.5 Incorporation of TiO ₂ flate membrane	15
2.6 Incorporation of TiO ₂ hollow membrane	19

Chapter 3	20
Experimental Methods	20
3.1 Materials used	20
3.2 Synthesis of polymer blend membrane	21
3.3 Synthesis of mixed matrix membrane	21
3.4 Characterization	22
3.4.1 Working Principle of FT-IR	22
3.4.2 Working principle of Scanning Electron Microscopy.	26
3.4.3 Working Principle of Tensile Testing Machine	28
3.4.4 Working Principle of X- rays Diffraction (XRD)	30
3.4.5 Working principle of water flux	36
3.4.6 Working Principle of UV spectroscopy	37
Chapter 4	38
Result and discussion	41
Testing techniques	41
4.1.1 FT-IR Spectroscopy Analysis	42
4.1.2 Tensile Testing Analysis	45
4.1.3 Scanning Electron microscopy (SEM) Analysis	48
4.1.4 Characterization	49
4.1.5 Water flux and salt rejection % testing	49
4.1.6 For polymer blend membrane Testing	51
4.1.7 Mixed salt water flux testing for poly amide-6(42 μ m)	56
Conclusion	61
Future Recommendation	66
Bibliography/References	67

List of Figures

Figure 1.1: Representation of the structure of MOFs	7
Figure 1.2 : Comparison of O=Ti=O with NH bond of Poly amide-6.	7
Figure 3.1 : Different modes of stretching and bending vibration	22
Figure 3.2 : Working Principle of FT-IR spectroscopy.	25
Figure 3.3 : Scattering of electron on interaction with matter.	26
Figure 3.4 : Schematic diagram of Scanning Electron Microscopy.	28
Figure 3.5 : The stress-strain behavior of several classes of materials	29
Figure 3.6 : Schematic diagram of Tensile Testing Machine	30
Figure 3.7 : Schematic diagram of Hollow fiber formation device	31
Figure 3.8 : Schematic diagram of water permeability testing	31
Figure 3.9 : Permeance molecule and retentate molecule /	32
Figure 3.10 : Schematic diagram of UV spectroscopy	35
Figure 4.1 : FT-IR of Pure PA/FA and TiO ₂ /PA/FA	39
Figure 4.2 : FTIR spectroscopy of pure polymer plus polymer having filler %	39
Figure 4.3 (a) : Tensile strength for membrane samples with different TiO ₂ %	42
Figure 4.3.(b) : Maximum tensile strength at 42μm thickness	43
Figure 4.4 : SEM images of polymer blend membrane without fillers	44
Figure 4.5 : SEM images of polymer blend membrane with fillers	45
Figure 4.6 : SEM images of porous polymer membrane with fillers	45
Figure 4.7: SEM images with different Concentration of filler.	46
Figure 4.8: SEM images with different Concentration of filler.	47
Figure 4.9: SEM images with different w/v	48
Figure 4.10 : XRD images of TiO ₂	49
Figure 4.11 : XRD images of pure PA , TiO ₂ , polymer with fillers %	49
Figure 4.12 : Different flux with different thickness	50

Figure 4.13 : UV spectroscopy images of polymer blend membrane	53
Figure 4.14 : UV spectroscopy images of polymer blend membrane	53
Figure 4. 15 : UV images of Calibration curve	54
Figure 4.16 : UV images of maximum salt rejection % of CaCl ₂	56
Figure 4.17 : Permeability of water in TiO ₂ /PA membrane at vary pressure	58
Figure 4.18 : Permeability of water (flux) in membrane at vary pressure	62

List of tables

Table 1.1: Composition of water in the world	1
Table 1.2 : Correlation between population and water consumption in tons	2
Table 2.1 : Literature review relating to MOFs	17
Table 2.2 : MOF and amino-modified MOF based mixed membrane	18
Table 2.3: Literature review of ZIFs and amino modified ZIFs	18
Table 2.4 : Literature review of ZIF based matrix membrane.	19
Table 3.1 : UV spectroscopy results	40
Table 3.2 : UV spectroscopy results	40
Table 4.1 : Flux and salt rejection % of CaCl ₂	51
Table 4.2 : UV testing of salt rejection % of CaCl ₂	52
Table 4.3 : Membrane types ,Flux and salt rejection %	57
Table 4.4 : CaCl ₂ & water flux , salt rejection % of different fillers	58
Table 4.5 : Different Salt rejection % of CaCl ₂ with different polymers	59
Table 4.6 : Comparison of flux and salt rejection % of both MMMs and PA	59
Table 4.7 : Flux and salt rejection % of both CaCl ₂ and MgCl ₂	61

List of Acronyms

FA	Formic Acid
PA	Polyamide-6
SEM	Scanning Electron Microscopy
UV	Ultra violet spectroscopy
MOF	Metal organic framework
ZIF	Zeolitic Imidazolate Framework
PVA	Poly-vinyl alcohol
PES	Polyether sulfone
FESEM	Field Emission SEM
FM	Flate membrane
HM	Hollow membrane
TDO	Titanium dioxide
PAN	Polyamide Nylon-6
THF	Tetra hydro furan
HCA	Hydrochloric acid
ED	Ethylene Diamine
PAAm	Poly allyl amine
PES	Poly ether sulfone
FESM	Field Emission SEM
UIO	University of Oslo
FA	Formic Acid
DMAC	Diethyl acid amide chloride
DMF	Dimethyle Formic acid
NA	Nitric Acid
CA	Cellulose Acetate
AC	Ammonium Chlorite
TEL	Tetra Ethylene lead
UTM	University of technology in Malaysia
PVA	Poly-vinyl alcohol

Chapter 1

Introduction

Background

Water is a major component for both industries and household use. The major portion of water is hydrogen, oxygen and essentials minerals such as calcium (Ca), Magnesium (Mg) and Sodium (Na). Other than the major components, water also contains a substantial amount of salts and impurities, such as magnesium chlorite ($MgCl_2$), calcium chlorite ($CaCl_2$), [1]. As an example, the composition of water is found in Malaysia which is summarized as follows (Table 1). According to Wausau et al, increased amount of minerals and salts is found to reduce the heating value of water, when compared to pure water. It has been proven from different experiments, where a range of water mixtures were taken with varying amounts of minerals and salts contained in those mixtures. It was seen that as the amount of salt and excess minerals increased, speed of heating and the heat generated from the reaction, decreased [2]. Moreover, as the world population increases, so does the global water demand. According to an estimate, the global population is projected to increase by a factor of 5.1% between 1990 and 2020, whereas the water consumption is projected to increase by 6.2% [3]. The water consumption and population was, then studied and a trend was established, which suggested that the population growth and water consumption both increased with each other as shown in Table 2 [4].

Table 1.1: Composition of water in the world [2]

Component	Volume percentage (vol %)
Water	70%
Fresh water	2.5%
Fresh water which is accessible	1.0%
Salt water	98%
Ice water	87%

Ground water	0.6%
Land water	0.3%

Table 1.2: Correlation between population (in thousands) and water consumption [4]

Year	Population	Water consumption
2000	676,037	1,460,284
2025 – Lower	774,902	1,805,297
2025 – Medium	793,659	1,953,477
2025 – Higher	812,144	2,101,007

Therefore, increased population requires increased water output, which in return requires increased water consumption. As our current water resources are already depleting very fastly. As indicated by a research carried out by N.A. Owen et al, there was an increase in water reserves in the early 1900s, especially from 1930 onwards. But, after 1990, the water Reserves started to deplete. This means that the amount of water taken out of the Reserves was more than the amount of in Reserves. After 1995, the Reserves have been depleting constantly, indicating a constant reduction in conventional water resources [5]. We have already seen that, increasing the amount of salts and minerals reduces the water output, so if we are to increase the output from conventional water resources, we must reduce the amount of salts and minerals in drinkable water being used. For the purpose of salts and excess minerals separation from various water, including natural water, we have a number of techniques, namely absorption through liquids, salt absorption on Solid surfaces [6], and membrane separation [7]. RO (Reverse osmosis) and UF(ultra filtration which have been most developed, and are considered most suitable for salt separation. Both these processes are widely used in the industry for salt separation. However, there are several drawbacks of these two techniques, and the main drawback is that both these techniques are energy-intensive (pressure supply) [8].Therefore, a less energy-intensive and a more energy-efficient process is required for the separation of salts and excess minerals, and research has been underway to find such a process or technique. Several decades of research have found that the most suitable process

which fulfils the required criteria is membrane separation, as it uses more or less energy than conventional salt separation techniques. Membrane processes use about 40-50% of the energy used by these thermally demanding techniques [9]. Also, membranes are a very promising technique to replace the conventional separation methods, because of their ease of manufacture, ease of integration into the existing industries and ease of scale-up [10]. Membranes are made of a number of materials, namely ceramics, metals, glass and polymers [11]. Of all these materials, we selected polymers as our desired medium for membrane fabrication, because of the economic advantage they serve as well as the ease with which a membrane can be fabricated using polymers [12]. Furthermore, of all the available polymers, we used polyamide polymers because of the efficient salt separation they give, owing to their flexible and fixed pores [13]. Finally, of all the polyamide polymers is selected because it is commercially available very easily and at a low cost but it is not much good for water permeation [14]. At first, when membrane salt separation was a new technique, single polymer membranes were used for this purpose. In a particular research work carried out by M.W. Tang et al, polyamide polymer membranes made with different solvents were tested for salt/water separation. These polyamide polymers membranes were fabricated from a range of solvents, including Formic acid(FA), toluene and xylene. The membranes showed a maximum salt/water selectivity of 36 and maximum water permeance of 42 G/ft²hm² (Water Permeation Unit) [15]. Another research work carried out by Chatterjee et al, polyether urethane and polyether urethane urea membranes were cast from solution of polymer in Di-MethylForm amide (DMF) and then tested for water permeation. The resulting membranes had a maximum salt/water and salt/water selectivity of 34 and 37 respectively [16]. Later on, as research progressed, it was seen that polymeric materials are limited in their separation performance for salt, as far as current membrane technology is concerned. So, new materials were required for improving salt separation performance [17]. Therefore, polymer blends membranes which were suggested for improving salt separation performance. The biggest advantage of blending membranes is, that they combine the favorable properties of two different polymers into one membrane. For example, one tough polymer can be combined with a highly permeable one, to give the benefits of high permeability as well as mechanical toughness [58]. A blend can also be the combination of highly porous polymer with a highly selective polymer

[61]. Membranes can also be formed from ceramics, metals or thermally-decomposed carbon. Some examples of such membranes include zeolites and carbon molecular sieves, which have tremendously higher selectivity and permeability as compared to polymeric materials. But, these materials present significant difficulties in the fabrication of continuous-phase membranes, which are free from crevices and other discontinuities, mainly because of their innate brittleness. Moreover, they are very costly to be made which put large barriers in the path of their use as a membrane material on their own [18]. Therefore, mixed matrix membranes comprising of a discrete inorganic phase and a continuous polymer phase are more favorable to be used for salt and excess minerals separation, instead of either purely polymeric or purely inorganic membranes. Moreover, mixed matrix membranes are much easier and cost-effective to produce as they are only a simple modification of the pure polymeric membrane [9]. Different types of filler particles were in use of membranes to improve their salts and excess minerals separation performance, such as TiO_2 , carbon molecular sieves and silica nano tubes. However, there are some emerging materials, which are also being tested, including carbon nano tubes and metal organic frameworks [19]. Of these materials, the most rapidly emerging are metal organic frameworks (MOFs) used in polymeric membranes. The main driving forces in this regard are the large number of combinations of linkers and metal ions that can be used, and the excellent porosity and adjustable pore sizes of MOFs [20]. Moreover, in addition to the ease of incorporation of MOF particles in membranes, thermal and chemical stability of the Materials must also be considered. Hence, it was found that some zeolitic imidazolate frameworks (ZIFs), a category of MOFs and titanium dioxide (TiO_2) exhibit superior thermal and chemical stability. Therefore, TiO_2 and ZIFs are a very favorable material to be used in membrane for salt and excess minerals separation [21].

1.1: Introduction to Polymer (PA-6) Blend Membranes

Polymer blends can be of two types, miscible and immiscible blends. In a miscible blend, all of the membrane components are dissolved in a single solvent [59]. Miscible polymer blends have a single phase, as they are completely dissolved in one another. Moreover, their properties are a function of composition alone. As far as properties like glass transition temperature and melting temperature are concerned,

there will be a single value as in a homo-polymer, but will depend on composition [62]. For making an immiscible blend, the different polymers are dissolved in a solvent system. This is because those polymers are not soluble in a single solvent [60]. In immiscible blends, however, the properties will depend on the phase distribution as well as the composition, and the different phases will act as separate pure polymers [62]. Therefore, the polymer blends can be used when we need to combine the advantages of two different polymers. Of these two types of blends, immiscible polymer blends have the advantage of giving us better control of membrane morphology. This means that we can change the composition of the blend to see what effect it has on the morphology of the final membrane [63].

1.2: Introduction to Mixed Matrix Membranes

Mixed matrix membranes are materials formed from the combination of polymeric materials and inorganic filler particles, which are inter-mingling to form one continuous matrix [12].

The inorganic filler particles may include TiO_2 [74], metal-organic frameworks [75] carbon molecular sieves [76] among others. These particles when incorporated into the structure of membranes are known to improve the separation performance of the original membranes as

will be explained in later chapters with adequate references to published text.

1.3: Introduction to Filler in Poly amid-6 &MOF (Metal organic Frame) works.

Metal-organic frameworks (MOFs) are a class of porous, polymeric solids which comprise of metal ions joined to one another by organic ligands. MOFs are mostly crystalline solids which can extend to one, two or three-dimensional structures depending on the way in which linkages are made. They can also be considered as co-ordination polymers, because of the repeating pattern of metal ions and organic ligands held in place by co-ordinate covalent bonds. These linkages between metal ions and organic linkers give rise to definite pores, which can trap certain gases, while letting others pass through, depending on the difference in pores sizes and the kinetic diameter of the gas molecules. MOFs are used in a number of applications. Some of

these applications can be summarized as follows:

- Salt separation, storage and capture [22]
- Salt sensing and detection, and advanced catalysis [23]
- Biotechnology and microelectronics [24].

Of these applications, we are more focused on the separation of salts using MOFs. As stated earlier, TiO₂ are a sub-category of metal organic frameworks (MOFs). They are so named, because of their resemblance in structure to zeolites (such as naturally-occurring and synthetic aluminosilicates). TiO₂ are formed by the linkage of transition metal They are so named, because of their resemblance in structure to zeolites (such as naturally-occurring and synthetic aluminosilicates). TiO₂ are formed by the linkage of transition metal ions (such as copper, zinc or cobalt) and imidazole linking groups, where the metal-imidazole-metal bond angle is similar to the silicon-oxygen-silicon (Si-O-Si) bond angle in zeolites (i.e. about 145°). From literature it was known that it gives very good result in case of salt separation from water as compared to other polymers due to many reasons which will discuss in the next chapter of characterization of poly amide-6 with optimize filler concentration .

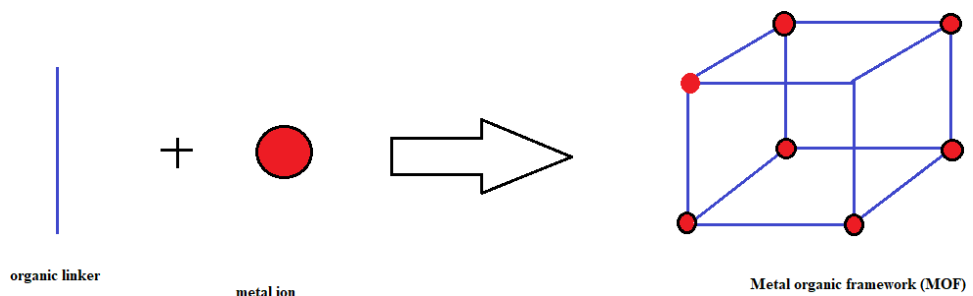


Figure 1.1: Representation of the structure of MOFs

They can also be considered as co-ordination polymers, because of the repeating pattern of metal ions and organic legends held in place by co-ordinate covalent bonds.

These bonds are not that much strong same like ionic or metallic bo

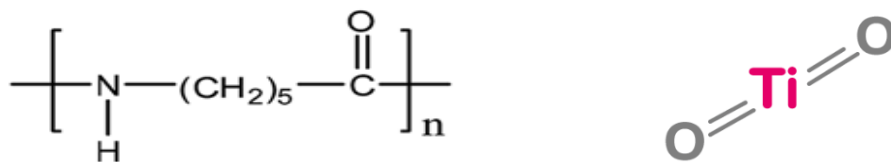


Figure 1.2 : The comparison of O-Ti-O bond in titanium dioxide with N-H bond in PA

1.4: Use TiO₂ in Poly amid-6 Membranes

As described earlier, TiO₂ have exceptional porosity and adjustable pores as well, so they can easily be used as filler particles dispersed in the bulk phase of a membrane, which is the main matrix. The main matrix or bulk phase may be polymeric, ceramic or membrane is to be subjected. TiO₂ are used in small quantities in the bulk membrane phase and have shown to exhibit excellent separation characteristics, even at such low concentrations.

1.5: Motivation

We want to better understand the effect of titanium di oxide on the water flux through a membrane; both TiO₂ and polymer blend membranes. Moreover, we also want to see the effect of changing the filler particles within the poly amid-6 membranes to increase the flux and salt rejection % . The aim of this work is to use amino-modified TiO₂ in a mixed matrix membrane as well as blend membranes, to improve the salt rejection %. This is done to compact the on-going water crisis by using the existing resources more efficiently. It also reduces the burden on the resources and limits the environmental impact of human activity. The objective o

Optimization and fabrication of blend poly amid-6 membranes

- To fabricate amino-modified TiO₂ based membranes and simple membrane.
- To investigate the effect of incorporating amino-modified TiO₂ to form a membrane and its advantage over high percentage of filler TiO₂ membrane
- To investigate the effect of blend membranes on the salt rejection % and flux of the membrane.
- Characterization of the resulting membranes using the following techniques

(1) Scanning Electron Microscopy (SEM)

(2) Fourier Transform Infra-red (FT-IR) Spectroscopy

- (3) Tensile Strength Testing
- (4) X-rays diffraction(XRD) of polymeric membrane
- (5) X-rays diffraction(XRD) of TiO₂
- (6) UV spectroscopy
- (7) Flux calculation in Lm²/hr
- (8) Salt rejection % at 237 nm wave length of CaCl₂ through UV spectroscopy
- (9) Finally, we intend to compare the separation performance of the blend membranes as well as the mixed matrix membranes, and recommend future advancements based on the results of that comparison.

1.6: Outline of the Thesis

1st Chapter details the introduction of polymer blends, their properties and their use in the separation of salt. This chapter also introduces titanium di oxide (TiO₂) and their uses in making mixed matrix membranes for salt and excess minerals separation. Then the amine-modified TiO₂ are also studied, and their use in mixed matrix membranes is explained. Finally, inorganic filler are also studied to see their use in membranes, as well as their amine-modified counterparts.

2nd Chapter includes examples of the research work carried out in the use of TiO₂, amine-modified TiO₂, TiO₂ and amine-modified TiO₂ in mixed matrix membranes, and the use of blend polymer membranes(poly amide) for salt separation.

MOFs also give excellent results we able to know from literature .

3rd Chapter summarizes the experimental techniques used to synthesize the mixed matrix and polymer blend membranes, and also the characterization techniques used to study their various physical and chemical properties.

4th Chapter studies the results obtained from different characterization techniques for all the synthesized membranes, and these results are then discussed in detail to explain their significance in my work.

Novelty was noticed in my work because of excellent results in both cases of flux and salt rejection % as well.

5th Chapter gives a concise summary of the entire work and also lists recommendations for future work of salt separation from water

Chapter 2

Literature Review

Salt must be removed from the water taken out from the reservoirs, as it reduces the water content of the overall water reserves. There are many different kinds of membranes used for this purpose, but polymer blend membranes and mixed matrix membranes are the most prevalent topics among researchers.

2.1: Applications of Blend Membranes

Polymer blends have long been reported in the industry and have been used in a number of applications like appliance housings, automotive interiors, wire and cable insulation [64]. However, in recent times, polymer blends have found applications in the fabrication of salt separation membranes [65]. These include both miscible and immiscible polymer blend membranes, which are both used in the formation of such membranes. The purpose of blend membranes is to incorporate certain functionalities into the membranes which would enhance its selective nature towards one particular component of the mixture to be separated. Therefore, in our case basic groups must be added in the membrane blend, as it is known that, when basic groups like -NH_2 and TiO_2 are present in any material, it would favorably adsorb salts. This technology is very vital in the removal of salts and excess minerals from water, which would otherwise contribute to climate change [30].

2.2: Use of polymer blend membranes for salt separation

For this reason, polymer blends are used, as polymer blends are an impressive technique for use in salt separation, and have many advantages over mixed matrix and inorganic particle (TiO_2) membranes. These advantages include simple design, easy fabrication and concerted effect of the blending components of a membrane

[66]. Miscible blends have been used for quite some time in the field of salt separation. Many research works have been published in this regard. Kapandaitakis et al reported the fabrication of a miscible poly-sulfone (PSf) and polyamide-6 (PA) blend membrane for the separation and permeation study of different pure water as well as

water mixtures. It was seen that the salted water, which do not chemically interact with the polymer components in the membrane such as CaCl_2 , MgCl_2 , NH_4Cl , and NaCl , show permeability values which are intermediate between the values for either pure PSf or pure PI. However, those salted water which do interact with the components (such as CaCl_2) would result in changes in permeability which cannot be explained by simple mixing equations. In this work, it is found that increasing the amount of PSf in the membrane decreases the plasticization effect of CaCl_2 which would mean that the membrane can be used for high pressure applications as well as for calcium chlorite- rich streams. The trend of Salt ion rejection (%) is noted for varying amounts of PA-6, and the Salt ion rejection(%) for $\text{NH}_4\text{Cl}/\text{MgCl}_2$, $\text{CaCl}_2/\text{NH}_4\text{Cl}$ and $\text{MgCl}_2/\text{CaCl}_2$ are in the range of 96-97, 95-93, 93-98 [67]. Moreover, Cai et al synthesized another miscible membrane comprised of polyamide (PA) and polyvinyl alcohol (PVA) using formic acid as a solvent. The resulting membrane gives a $\text{CaCl}_2/\text{NH}_4\text{Cl}$ Salt ion rejection(%) of 95.8 and $\text{MgCl}_2/\text{NH}_4\text{Cl}$ Salt ion rejection (%) of 98 [68]. As stated earlier, there is another type of polymer blend membrane, namely immiscible blend membranes. Lots of research is currently being done in this regard, and many publication are being made on this topic. Wang et al synthesized an immiscible blend membrane consisting two different grades of polyether sulfone (PES), namely Victrex 4802 P and Radel A-300 dissolved in a solvent system of N- methyl-2-pyrrolidone (NMP) and alcohols (methanol, ethanol, 1-propanol, 1-butanol, 1-pentanol, ethylene glycol, diethylene glycol). The fabricated membranes give a maximum Salt ion rejection (%) for $\text{NH}_4\text{Cl}/\text{CaCl}_2$ of around 94.98 [69]. In another research work carried out by J. Li et al, Poly amide-6 (PA) and polyethylene glycol (PEG) blend membranes were fabricated in a solvent system of dichloromethane and tetrahydrofuran. The resulting membrane is found to have a maximum Salt ion rejection(%) for PA membrane containing 1% TiO_2 having molecular weight (MW) of 85000, and the values for $\text{CaCl}_2/\text{NH}_4\text{Cl}$ and $\text{MgCl}_2/\text{NH}_4\text{Cl}$ Salt ion rejection(%) come out to be 96.2 and 94.3 [70]. After studying different examples of both the miscible and immiscible blends, their advantages and the benefit of incorporating amine group into the structure, we have found out that using a polyamide/ Formic Acid blend membrane would have the advantage of amine group addition as well as the added Favor of Poly amide-6, which is readily available. Therefore, this could be a viable option is poly amide-6, which is readily available. Therefore, this could be a viable

2.3: Use of Titanium di oxide for separation

As stated earlier, in the field of salt separation, metal organic frameworks have been used for several decades. This application of MOFs is due to some favorable properties of MOFs, which will be explained here. The process employed for salt separation when using MOFs only, is through selective adsorption of one salt with respect to another [27]. In this regard, Chen et al synthesized a biological metal-organic framework (Bio-MOF-11) and tested its adsorption capacity for CaCl_2 , NH_4Cl and MgCl_2 . The adsorption salt rejection % for $\text{NH}_4\text{Cl}/\text{MgCl}_2$ in the salt mixture water is found to be between 94 and 96, whereas the salt ion rejection (%) for $\text{CaCl}_2/\text{MgCl}_2$ in the respective salt mixture water is found to be in the range of 90 to 97 [28]. In another work, Li et al synthesized and tested the salt of a zinc benzene-tri-benzoate metal organic framework (MOF), namely MOF-7. The salt rejection characteristics showed that CaCl_2 is adsorbed salt rejection % than MgCl_2 with a salt rejection % of 96.8 Where as the maximum TiO_2 uptake is at a value of 1.5 wt% [29]. Amine-functionalized titanium dioxide are very suitable for calcium chlorite adsorption, because of the favorable affinity between basic amine groups and acidic calcium chlorite, as stated earlier. A particular work in this field was carried out by McDonald et al. In this work, they synthesized a special kind of MOF with general formula $\text{M}_2(\text{dobpdc})$ using 4,4-dioxido-3,3-biphenyl di-carboxylate (dobpdc), which was then functionalized using N,N-dimethylethylenediamine (mmen) to form the amine functionalized MOF. Mmen- $\text{Mg}_2(\text{dobpdc})$. The resulting MOF gives a $\text{CaCl}_2/\text{MgCl}_2$ adsorption salt rejection % of 98.5 and a $\text{CaCl}_2/\text{NH}_4\text{Cl}$ adsorption salt rejection of 96.5 [31]. A lot more work was carried out in this aspect, after the discovery of the superior carbon capture ability of MOFs, after amine- fictionalization. In one such work carried out by Wang et al, a MOF named MIL- 101 was modified using tetra-ethylene-pentamine (TEPA) to form TEPA-MIL-101. Both un-modified and modified MOFs were used for CaCl_2 and MgCl_2 separation. The subsequent product showed an increase in CaCl_2 adsorption capacity whereas the adsorption capacity of MgCl_2 drastically dropped, and the adsorption salt rejection % of $\text{CaCl}_2/\text{MgCl}_2$ was enhanced from 96.77 to 98.2 due to amine functionalization [32]. A lot more work was carried out in this aspect, after the discovery of the superior carbon capture ability of MOFs, after amine- fictionalization. In one such work carried out by Wang et al, a MOF named MIL- 101 was modified using tetra-ethylene-pentamine (TEPA) to form

TEPA-MIL-101. In one such work carried out by Wang et al, a MOF named MIL-101 was modified using tetra-ethylene-pentamine (TEPA) to form TEPA-MIL-101.

2.4: Use of ZIFs for salt adsorption and separation

With the passage of time, more and more materials were synthesized and tested for their salt adsorption and separation performance. A breakthrough was made when a special class of porous materials was found to have exceptional characteristics. These materials are called Zeolitic imidazolate frameworks (ZIFs). Zeolitic imidazolate frameworks (ZIFs) are a class of metal organic frameworks, which consist of a crystal structure based on alumina-silicate zeolites with the tetrahedral alumina-silicate and bridging O atoms replaced by transition metal ions and imidazolate linkers respectively [33]. An example of this can be shown in a work carried out by Prakash et al, in which computational analysis based on experimental data, of Ti uptake capacity of TiO₂ and ZIF-100 was done, and it was found that the adsorption capacity of the ZIFs was 0.25 and 1 wt% respectively [34]. ZIFs are known to adsorb salts reversibly and the adsorption is weak. This was shown by a research work carried out by Saracco et al, where salt from water is rejected adsorbed by co-ordination with the outer Co (II) ions in a Co-ZIF-67 to form a superoxo species, which can be desorbed using light. This shows that not only will the salt be adsorbed from salt mixture water, it can be easily separated from ZIF as well [35]. Just like ordinary MOFs, the performance of ZIFs can also be improved and enhanced by amine-modification. Many researches have been published in this regard. An example of this was the research work carried out by Binti-Yahya et al, in which they synthesized amino-functionalized ZIF-8, and the amine modification was carried out using the wetness impregnation method, with two kinds of amine-containing compounds namely tetra-ethylene-pentamine (TEPA) and penta-ethylene-hexamine (PEHA). In this work, the adsorption capacity of amine-modified ZIF-8 was measured, and was compared with the un-modified ZIF-8. The CaCl₂ adsorption capacity of the amine-modified ZIF-8 was measured to be 2.9983 mmol/g, and after amine-modification, the CaCl₂ adsorption capacity was increased up to 99.6% [36]. Another work carried out by Zhang et al detailed the advantages of amine-modification on carbon capture. Here, ZIF-8 is subjected to a process called “post-synthetic modification”. In this process, amine groups are incorporated into ZIF-8 using ethylene di-amine, and its adsorption capacity is greatly enhanced, whereas the CaCl₂ salt rejection % goes up to 93.5 at 73 bar and 96.9 at 78.5 bar

[37]. Similarly, in the case of MOFs, lot of research is being done, which is much matching with poly amide-6 having specific fillers.

2.5: Incorporation of MOFs in membranes

For a long time, polymeric membranes had been used for salt separation, but there is always a limit to which, such membranes can be used for salt separation. However, when mixed matrix membranes are formed, they would combine the advantages of inorganic fillers and organic polymeric membranes [38]. Similarly, in the case of MOFs, lot of research is being done with MOFs incorporated in polymeric membranes. In one such work, Basu et al prepared a Matrimid based mixed matrix membrane, with different loadings of a MOF called MIL-53(Al) ranging from 0- 30%. Results showed that the increase in loading of MIL-53 gives an increase in CaCl_2 permeance up to 38%, whereas the $\text{CaCl}_2/\text{NH}_4\text{Cl}$ salt rejection % also increased and was in the range of 28-35 [39]. In one other research work, Perez et al synthesized Matrimid based membrane with MOF-5 as filler in its structure. The incorporation of MOF-5 in the membrane increased the permeability of the water by 97%. The $\text{CaCl}_2/\text{MgCl}_2$ salt rejection % was found to be in the range of 96 to 97, and $\text{CaCl}_2/\text{NH}_4\text{Cl}$ salt rejection % was found to be 94 to 95 [40]. Similarly, as stated earlier, when MOFs are modified with amine groups, they can capture carbon dioxide more readily. When these amine-modified MOFs are used in membranes, they would naturally improve the permeation and salt rejection % of CaCl_2 over other salts. This property of amine-modified MOF based mixed matrix membranes (MMMs) was exploited for CaCl_2 separation from water and flue water in a number of research works. In one particular research work carried out by Zornoza et al, the research team synthesized MIL-53 (Al) and modified it with amine groups to form NH_2 -MIL-53 (Al), which was in turn integrated into a poly-sulfone membrane to form the resulting matrix. This membrane gives much better separation of CaCl_2 over H_2O and gives a maximum $\text{CaCl}_2/\text{NH}_4\text{Cl}$ salt rejection % of 95 [41]. In another similar work, M.W. Anjum et al synthesized mixed matrix membranes (MMMs) composed of zirconium terephthalate UiO-66 as the filler with Matrimid as the base polymer, the MOF was functionalized by adding amine groups from 2-aminoterephthalic acid and 4-aminobenzoic acid. This resulting membrane had better CaCl_2 separation as compared to unfilled (with no MOF) Matrimid membrane, and gives a maximum $\text{CaCl}_2/\text{NH}_4\text{Cl}$ salt rejection % of 97.7. This property of amine-modified MOF based mixed matrix

membranes (MMMs) was exploited for CaCl_2 separation from water and flue water in a number of research works [42].

2.6: Incorporation of TiO_2 and ZIFs in membranes

Just like ordinary MOFs, ZIFs have also been used in membranes for facilitating salt separation. Infinite research is being carried out in this regard, to form a suitable blend for most effective gas separation. One research work carried out by Li et al, TiO_2 was combined with poly (amide-b-ethylene oxide) (Pebax® 1657, Arkema) to form a mixed matrix membrane. The membrane thus formed has a maximum H_2O permeability ($P_{\text{H}_2\text{O}}$) up to 45 barrers, $\text{CaCl}_2/\text{MgCl}_2$ salt rejection % up to 97, and $\text{CaCl}_2/\text{NH}_4\text{Cl}$ salt rejection % up to 90 [43]. In one research conducted by Bux et al, an ethane/ethane mixture was separated by adding TiO_2 as filler on top of a titania-alumina support layer, which acted as the main membrane phase. This membrane shows an ethene/ethane salt rejection % of 92.8 and 95.4 at a pressure of 71 and 86 bar respectively. The fairly low salt rejection % of salt over water is primarily due to two competing salt rejection %, superior salt absorption salt rejection % and superior salt diffusion salt rejection % [44]. If the structures of TiO_2 are augmented by adding amine groups, and then these amine-impregnated ZIFs are included in the membrane structure, they can also introduce several desirable CaCl_2 separation properties within the structure. In one such study, Nordin et al synthesized the zeolitic imidazolate framework ZIF-8 and TiO_2 , which was then modified using ammonium hydroxide. The resulting amine modified ZIF-8 was then dispersed in the base polymer membrane made of poly-sulfone. The resulting membrane is tested for its permeability and selectivity with $\text{CaCl}_2/\text{NH}_4\text{Cl}$ mixture, the $\text{CaCl}_2/\text{NH}_4\text{Cl}$ salt rejection % was found to be in the range of 95 [46]. Another research on the CaCl_2 separation from salt mixtures water using amino-modified ZIF based membranes was carried out by Huang et al, who synthesized and modified ZIF-90 using amino propyltriethoxysilane (APTES). The amino-modified ZIF-90 membranes. were synthesized by coating the α -alumina.

The resulting membrane is then tested for salt separation .The $\text{CaCl}_2/\text{NH}_4\text{Cl}$ salt rejection was up to 94.7 in the work [46]. Another research on the CaCl_2 separation from salt mixtures water using amino-modified ZIF [46]. The testing is carried out at different pressures, just like in the case of single salt mixture permeation testing which come out in the form of a UV (ultra violet) spectroscopy but this one shows 73% salt rejection which is not satisfaction or match with literature review. The salt rejected through this way is 97.5 % and flux through this way is 40 and 41 Lm^{-2}/hr . The above graph shows 73% salt rejection which not enough is because our literature shows that salt rejection % should above than 95% .Through UV graph of calibration. The salt rejected through this way is 97.5 % and flux through this way is 40 and 41 Lm^{-2}/hr .

Table 2.1: MOF and amino-modified MOF based mixed membranes

Polymer	Filler	Salt ion rejection(%)	References
Matrimid	MIL-53 (Al)	$\text{NH}_4\text{Cl}/\text{MgCl}_2$ 92.76/96.71	[39]
Matrimid	MOF-5	Iodine Salt/ CaCl_2 93.2/96.67	[40]
Polysulfone	NH_2 -MIL-53	$\text{CaCl}_2/ \text{NH}_4\text{Cl}$ 89.67/91.87	[41]
Matrimid	Zirconium terephthalate UiO- 66	$\text{NaCl} /\text{MgCl}_2$ 95.5/93.5	[42]
Poly amide-6	Poly amide with filler of 0.5 %	$\text{CaCl}_2=94.56$	[43]
Poly amide	1.5 % filler	$\text{MgCl}_2=96.34$	[44]
PVA	0.5 % filler	$\text{MgCl}_2=94.5$	[45]

Table 2.2: Literature review relating to MOFs and amino-modified MOFs

Matrix material	Filler	Salt ion rejection(%)	Reference
Titania-alumina support	ZIF-8	Ethene/ethane = 2.8	[46]
Polysulfone	ZIF-8 modified	CaCl ₂ /NH ₄ Cl = 95-93	[47]
Poly amide polymer	TiO ₂ modified	CaCl ₂ =94	[48]
Poly sulfone polymer	TiO ₂ modified	CaCl ₂ =97	[49]
Poly ether sulfone polymer	TiO ₂ modified	CaCl ₂ =96	[50]
PEG polymer	TiO ₂ modified	CaCl ₂ =95	[51]
α -alumina support	APTES-modified ZIF-90	CaCl ₂ /NH ₄ Cl = 94.7	[52]
PA-6	TiO ₂ (0.5 %)	CaCl ₂ =97.5	[53]

Firstly, we have the spectrum of the membrane sample made of pure Formic acid. It contains a perfectly bell-shaped inverted peak at the wave number value of 3487.71 cm⁻¹, which is due to the stretching vibrations of the N-H bond. The testing is carried out at different pressures, just like in the case of single salt mixture permeation testing which come out in the form of a UV (ultra violet) spectroscopy but this one shows 73% salt rejection which is not satisfaction or match with literature review. The salt rejected through this way is 97.5 % and flux through this way is 40 and 41 Lm²/hr. The above graph shows 73% salt rejection which not enough is because our literature shows that salt rejection % should above than 95% .Through UV graph of calibra ¹⁷

Firstly, we have the spectrum of the membrane sample made of pure Formic acid. It contains a perfectly bell-shaped inverted peak at the wave number value of 3487.71 cm⁻¹, which is due to the stretching vibrations of the N-H bond in poly amide-6 due to

presence of fillers. The salt rejected through this way is 97.5 % and flux through this way is 40 and 41 Lm⁻²/hr. The testing is carried out at different pressures, just like in the case of single salt mixture permeation testing which come out in the form of a UV (ultra violet) spectroscopy but this one shows 73% salt rejection which is not satisfaction or match with literature review. Nordin et al synthesized the zeolitic imidazolate framework ZIF-8 and TiO₂, which was then modified using ammonium hydroxide. The resulting amine modified ZIF-8 was then dispersed in the base polymer membrane made of poly-sulfone. The resulting membrane is tested for its permeability and selectivity with CaCl₂/NH₄Cl mixture, the CaCl₂/NH₄Cl salt rejection % was found to be in the range of 95[46]

Table 2.3: Literature review of polymer blend membranes

Metal organic Frameworks (MOFs)	Salt ion rejection(%)	References
Bio-MOF-11	NH ₄ Cl/MgCl ₂ = 94-96 NaCl/ NH ₄ Cl = 90-92	[54]
MOF-17	NH ₄ Cl/CaCl ₂ = 1.8	[55]
Mmen-MgCl ₂ (dobpdc	CaCl ₂ /NaCl =89.5/92.5 NaCl /MgCl ₂ = 96.5/92.5	[56]
TEPA-MIL-101	Iodine Salt/ CaCl ₂ = 90.2/91.67	[57]
Poly amide-6	CaCl ₂ =97.5	[58]
Poly amide-6 (0.5%)	CaCl ₂ =97.5	[59]
Poly amide-6 (1.75%)	CaCl ₂ =93.5	[60]
Poly amide-6 (1%)	MgCl ₂ =94.5	[61]
Poly amide-6 (1.5%)	MgCl ₂ =96.5	[62]

Chapter 3

Experimental

3.1: Materials Used

Poly amide (PA-6), $M_n = 85,000$ g/mol by Gel Permeation Chromatography (GPC) was obtained from Sigma-Aldrich, St. Louis, MO, USA. Poly-(allylamine) solution (average $M_w \sim 65,000$ g/mol, 20 wt% in Formic Acid) was procured from Sigma-Aldrich, St. Louis, MO, USA. Poly-ethylene glycol, $M_w = 1000$ g/mol, was procured from Siheung, Daejung, Korea. Ultra-pure acetone ($M_w = 58.08$, 99% purity GC) was purchased from Sigma-Aldrich, and used without further purification, and de-ionized water was obtained from within the laboratory. As-prepared amino-modified TiO_2 was obtained from another research student within the research group. For the purpose of water permeation testing, $CaCl_2$ (96.999 vol%), commercial grade $MgCl_2$ (97.995 vol%) and $CaCl_2/NH_4 Cl$ (10:90 by volume) salt mixture water, PEG(Poly ethylene glycol was also used with titanium dioxide.

We made different solution by using TiO_2 of different wt % (0.5, 0.75 , 1 ,1.5) in 20 wt% polyamide in Formic acid .Similarly for calibration curve we use $CaCl_2$ salt in Distilled water by making (0.1mm/L ,0.2mm/L ,0.4mm/L ,0.6mm/L , 0.8mm/L , 1mm/L) which give us straight line in UV spectroscopy .

3.2: Synthesis of Polymer Blend Membranes

For the fabrication of polymer blend membranes, the concentration of PA and Formic acid in a solution containing a formic acid and weak hydrochloric acid solvent system, is to be optimized. Formic acid is used in this solvent system to dissolve PA-6. But before that, the concentration of the two solvents in the system is to be optimized. It is found that only solvent systems containing 98% formic acid and 2% hydrochloric acid by having 0.5% titanium dioxide , form membranes which are flexible enough to be tested and used. However, PEG of MW 1000 is still needed for the membranes to be flexible enough for further use. But, TiO_2 gives rise to the formation of pores when used in larger quantities. So, we had to optimize the amount of used TiO_2 , such that it did not form porous membranes, while still granting the membrane flexibility We used

0.5%, 1% and 1.5% TiO_2 in the PA/formic acid. Of these, the membranes containing 0.5% TiO_2 were the only ones which were acceptably porous poly amide-6 membrane, after they were tested for water permeation and rejection of salt %. The final polymer blend membranes were synthesized by first adding 20% w/v PA-6 in formic acid. In this blend, varying amount of TiO_2 ranging from 0.5% to 2% (filler-to-polymer) was incorporated because of high concentration of solute then the solution was cast on solvent rinsed petri dishes, kept in the oven at 40°C for one hour. These membranes were tested for water permeation and salt separation, as well as characterized accordingly.

3.3: Synthesis of Mixed Matrix Membranes

Membranes were fabricated using the solution casting method. For the preparation of casting solution, 20% w/v (polymer-to-solvent) of poly amide (PA) was added to 10 ml of formic acid, and left to stir overnight on a magnetic stirrer. Separately, different percentages of as-synthesized amino-modified TiO_2 were added to 10 ml of formic acid, ranging from 0.5% to 2% w/w (filler-to-polymer) with an increment of 3% for each subsequent sample. This solution of TiO_2 in formic acid is then subjected to sonication, using sonication probe, for 4 hours. Then, the two separate solutions were combined and further stirred overnight. The resulting solution was then sonicated for another 35-45 minutes, before being cast onto solvent-rinsed petri dishes (solvent used distilled water mostly). Once cast, the solution was left under atmospheric conditions for another 35-45 minutes, for solvent evaporation. Then, for proper evaporation of solvent, it was transferred to a preheated vacuum oven and left for 3-4 hours at 40°C. The different membrane samples made, were then tested for water permeation for both single and mixed salts. For analysis of permeate from salt mixed water, Ultra violet spectroscopy (UV) is used. The membranes are then characterized using Fourier Transform Infra-red (FT-IR) spectroscopy, Scanning Electron Microscopy (SEM) and Ultimate Tensile Testing analysis also XRD to check inorganic particles (TiO_2) presence. This solution of TiO_2 in formic acid is then subjected to sonication, using sonication probe, for 4 hours. Then, the two separate solutions were combined and further stirred overnight.

3.4: Testing and Characterization

3.4.1: Working principle of FT-IR Spectroscopy

When infra-red radiation is incident on matter, it is absorbed by the matter. There are several vibrational states of a molecule. Once the radiation is absorbed, it causes the molecules to go from the ground state to the excited state, which means that the molecule goes to a higher vibrational state. The amount of energy needed to transfer the molecule to that higher state is proportional to the wavelength of the radiation absorbed. Every particular molecule has several functional groups in it, each of which absorbs radiation in a different specific wavelength, which is then called the *fingerprint* of that functional group. All the characteristic absorption peaks of each functional group combine to form the spectrum.

of that particular molecule, which is generated and studied using the FT-IR spectrometer vibration [53].

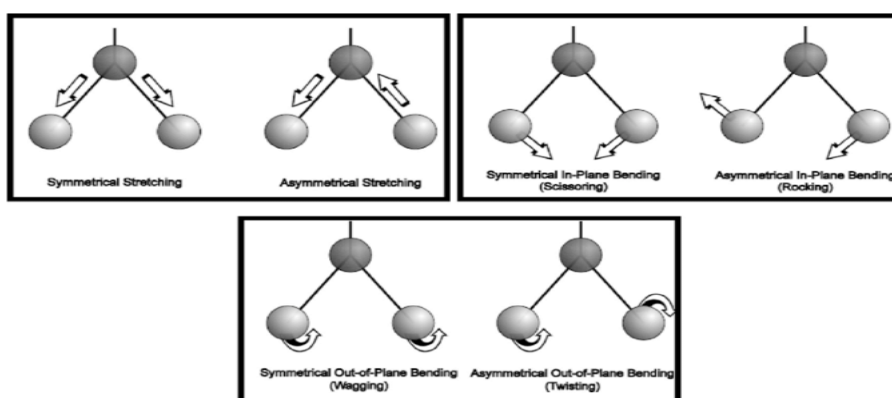


Figure 3.1: Different modes of Stretching and Bending

FT-IR stands for Fourier Transform Infra-Red spectroscopy. It is a major analytical technique for the detection and determination of the identity of functional groups in a sample. When infra-red (IR) radiation is incident onto a sample, some radiation is absorbed by the sample, while some part of it passes through it. Whether we study the absorbance or transmittance of radiation, there is a certain characteristic spectrum, which results from a particular material. This is called the *fingerprint* of the sample. A FT-IR spectrometer consists of the following parts:

- IR source
- Beam splier
- Fixed and movable mirrors
- Sample cell

- Detector

Inside an FT-IR spectrometer, an IR source generates infra-red radiation, which then is incident into a beam splitter. Here, the beam is split into two parts, one goes into the fixed mirror while the other goes into the movable mirror. This is done to take out only that portion of the IR spectrum, which is necessary for our analysis. The resulting beam is then recombined into one beam, and now contains only that region of IR which is required. This resulting beam then goes into the sample cell, where the absorbance of radiation takes place. Then, according to our requirements, the resulting spectrum is sent to the detector. The detector output is converted into interpretable spectra. FT-IR uses interferometry to record information about the material in the form of *interferograms*, and Fourier Transform is used to convert these interferograms into spectra which is used to identify and quantify the material.

The testing is carried out at different pressures, just like in the case of single salt mixture permeation testing which come out in the form of a UV (ultra violet) spectroscopy but this one shows 73% salt rejection which is not satisfaction or match with literature review. The salt rejected through this way is 97.5 % and flux through this way is 40 and 41 Lm²/hr. The above graph shows 73% salt rejection which not enough is because our literature shows that salt rejection % should above than 95% .Through UV graph of calibration. Firstly, we have the spectrum of the membrane sample made of pure Formic acid. It contains a perfectly bell-shaped inverted peak at the wave number value of 3487.71 cm⁻¹, which is due to the stretching vibrations of the N-H bond. The testing is carried out at different pressures, just like in the case of single salt mixture permeation testing which come out in the form of a UV (ultra violet) spectroscopy but this one shows 73% salt rejection which is not satisfaction or match with literature review. The salt rejected through this way is 97.5 % and flux through this way is 40 and 41 Lm²/hr. The above graph shows 73% salt rejection which not enough is because our literature shows that salt rejection % should above than 95% .Through UV graph of calibration. Firstly, we have the spectrum of the membrane sample made of pure Formic acid. It contains a perfectly bell-shaped inverted peak at the wave number value of 3487.71 cm⁻¹, which is due to the stretching vibrations of the N-H bond.

When an electron beam is introduced into a column of the Scanning Electron

Microscope, it does not encounter any atoms of any gas or liquid, in the atmosphere because a vacuum is established in that column. There is no interaction of electrons with matter, until it encounters the highly dense solid material. When the electron beam is incident on a sample, it transfers some of its energy to the molecules in the sample. This causes it to be reflected at an angle to its original well-defined trajectory. There is no interaction of electrons with matter, until it encounters the highly dense solid material. When the electron beam is incident on a sample,

The below is the working principle of FT-IR used for functional groups.

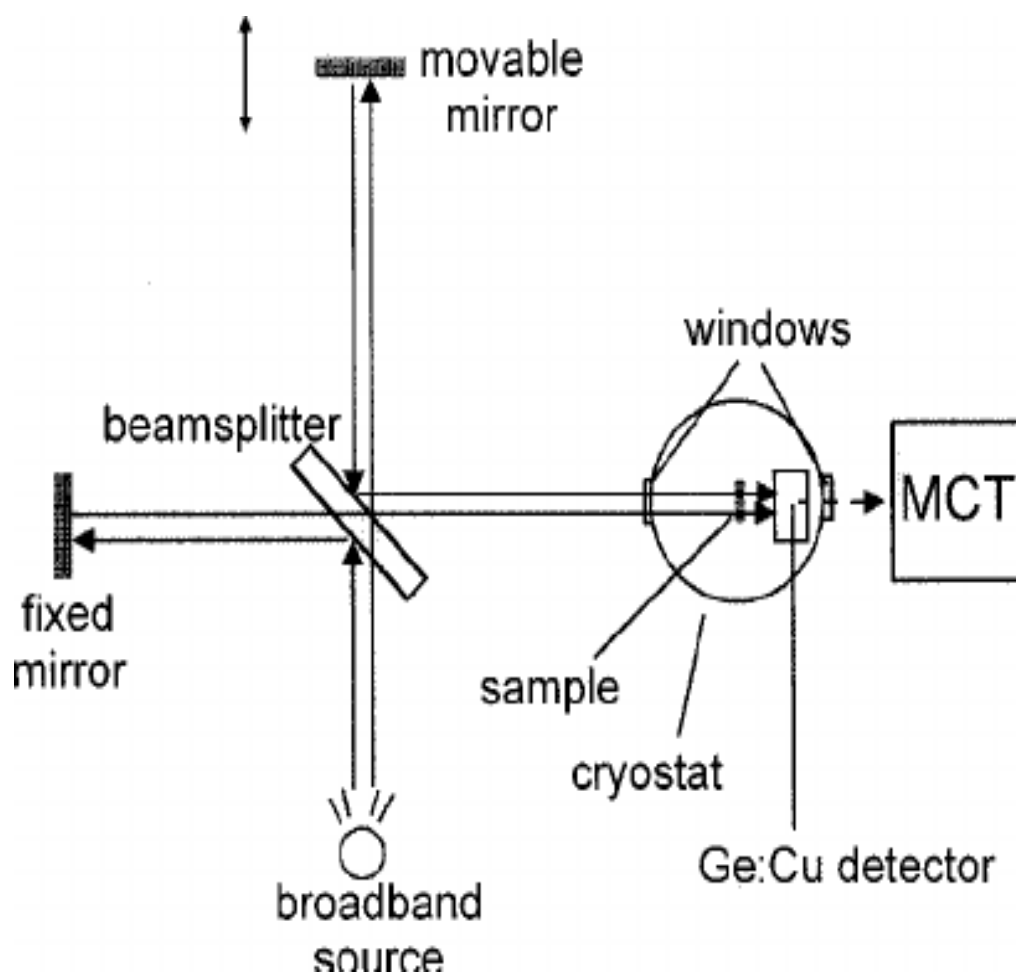


Figure 3.2: Working principle of FT-IR spectroscopy [47]

FT-IR Spectroscopy was carried out using Perkin-Elmer Spectrum 100 FT-IR spectrometer. The analysis was carried out in the wave number range of $4000\text{-}400\text{ cm}^{-1}$ and at a resolution of 4 cm^{-1} . The membrane samples were tested by cutting out a suitable sized sample and fitting it into the sample cell of the spectrometer. After

fitting the membrane sample into the sample cell, IR radiation was then incident on the sample membrane. This resolved the membrane into its functional groups, which are then studied when the spectrum is formed. The analysis was carried out in the wave number range of $4000\text{-}400\text{ cm}^{-1}$ and at a resolution of 4 cm^{-1} . The membrane samples were tested by cutting out a suitable sized sample and fitting it into the sample cell of the spectrometer. The membrane samples were tested by cutting out a suitable sized sample and fitting it into the sample cell of the spectrometer

3.4.2: Working principle of Scanning Electron Microscopy

The science behind the process of scanning electron microscopy (SEM) is the interaction of electrons with specimen material. When an electron beam is introduced into a column of the Scanning Electron Microscope, it does not encounter any atoms of any gas or liquid, in the atmosphere because a vacuum is established in that column. There is no interaction of electrons with matter, until it encounters the highly dense solid material. When the electron beam is incident on a sample, it transfers some of its energy to the molecules in the sample. This causes it to be reflected at an angle to its original well-defined trajectory. This results in the formation of back-scattered electrons, secondary electrons and X-rays. These interactions give us much needed information about the topography, composition, crystal structure and the presence of any electrical and magnetic fields. All these interactions result in the scattering of electrons, which can be classified into two main types, elastic and inelastic scattering

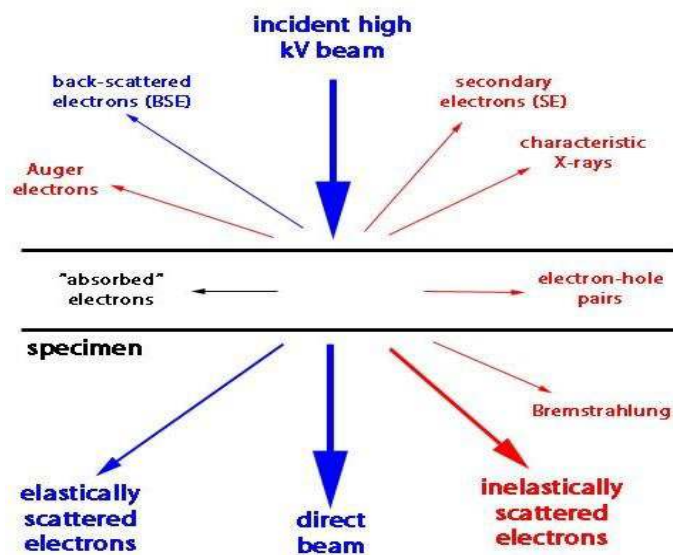


Figure 3.3: Scattering of electrons on interaction with matter [55]

[54], as shown in Figure. There is no interaction of electrons with matter, until it encounters the highly dense solid membrane. Scanning Electron Microscopy (SEM) is used to study the morphology of membranes. It can also be used to study the presence and distribution of pores throughout the membrane. For this purpose, electrons are produced by an electron gun, passed through accelerating voltage which causes them to travel quickly down a column, through many lenses and apertures, The lenses and apertures are used to produce a focused beam of electrons which ultimately hits the sample. The sample is placed in the chamber area. As the electrons are supposed to be focused onto the sample, therefore both the column and the sample chamber must be under vacuum, which can be brought about by a series of pumps. The beam is focused on to a particular area of the material by using scan coils, located directly above the objective lens. The scanning of the electron beam over that region of the sample, helps us in studying the properties of a particular portion of the sample. Different signals are given out from this process which are then captured and analysed by suitable detectors. The main components of the Scanning Electron Microscope (SEM) are:

- Electron source
- Column and electromagnetic lenses
- Electron detector
- Sample chamber
- Display screen

The schematics of the Scanning Electron Microscope can be shown as follows. The testing is carried out at different pressures, just like in the case of single salt mixture permeation testing which come out in the form of a UV (ultra violet) spectroscopy but this one shows 73% salt rejection which is not satisfaction or match with literature review. The testing is carried out at different pressures, just like in the case of single salt mixture permeation testing which come out in the form of a UV (ultra violet) spectroscopy but this one shows 73% salt rejection which is not satisfaction or match with literature review. The salt rejected through this way is 97.5 % and flux through this way is 40 and 41 Lm^{-2}/hr . The above graph shows 73% salt rejection which not enough is because our literature shows that salt rejection % should above than 95% of salt rejection of CaCl_2 than MgCl_2 one mixture of different salt water with maximum salt rejection % that is 97.5 % through UV spectroscopy of calibration curve. .

Through UV graph of calibration. Firstly, we have the spectrum of the membrane sample made of pure Formic acid. It contains a perfectly bell-shaped inverted peak at the wave number value of 3487.71 cm^{-1} , which is due to the stretching vibrations of the N-H bond.

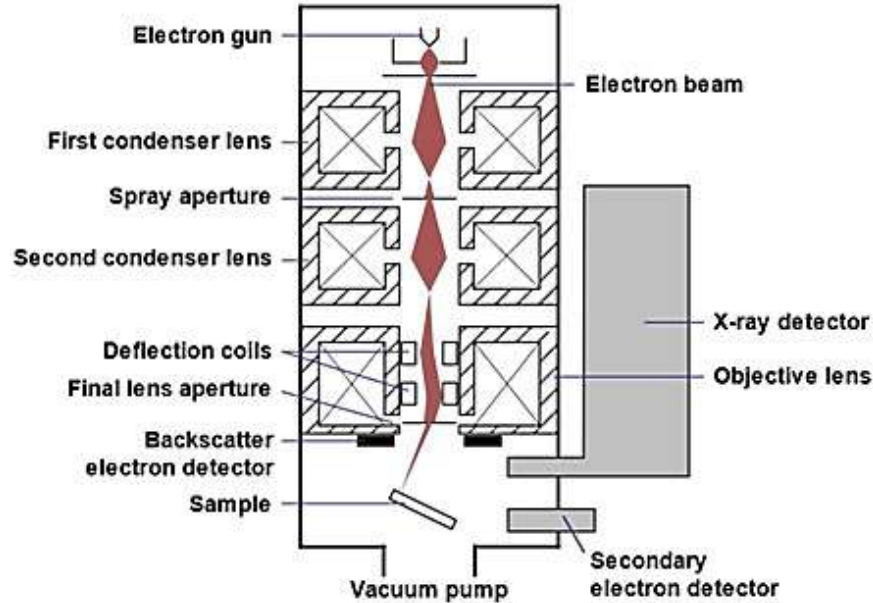


Figure 3.4: Schematic diagram of Scanning Electron Microscope [48]

SEM analysis is performed by using TESCAN MAIA3 Field Emission Scanning Electron Microscopy (FESEM) for determining the morphological properties of the membrane samples. All the membrane samples having 0.5%, 1%, 1.5% and 2% w/w (filler-to-polymer)

amino-modified $\text{TiO}_2/\text{PA}/\text{formic acid}$ membranes are characterized using this arrangement for the study of their pore distribution and pore structure. The analyses are performed at an accelerating voltage of 2 kV and magnifications of 5000x, 10,000x, 15,000x, 20,000x, 25,000x and 30,000x. The final SEM images are then studied to determine their surface features.

3.4.3: Working principle of Tensile Testing Machine:

Tensile strength of a material is the maximum stress that a material can withstand until it breaks. There are different classes of materials, based on their mechanical strength. These include glassy and rubbery materials. The classification into these two categories depends on their stress-strain behaviour. The glassy materials are rigid and brittle, whereas the rubbery materials are mostly flexible. The stress-strain behaviour

of various types of materials is shown in Figure 7 (on the next page). Here we deal with a rubbery membrane which is flexible and also porous in nature for water permeation and salt rejection %.

In this figure, the curve shows that brittle (glassy) materials show a high tensile strength, which is the end point of each curve here, but show only a small amount of strain. Whereas, the more flexible rubbery material shows a large strain, but a significantly lower tensile strength.

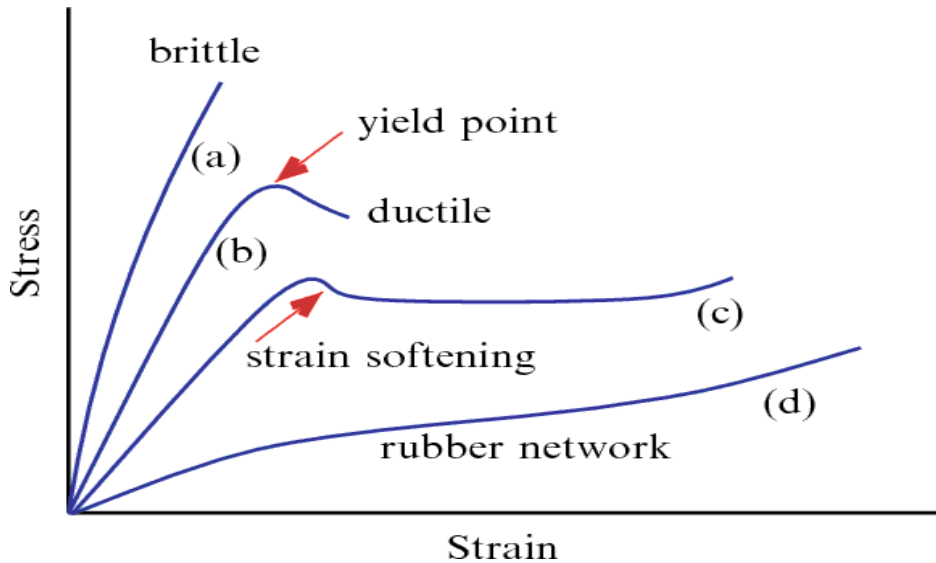


Figure 3.5: The stress-strain behavior of several classes of materials [56]

The Tensile Testing Machine can be used to find out the tensile strength of the membrane materials. This machine consists mainly of a load which is connected to a movable upper jaw, to which one end of our test material is clamped. On the other end, is the fixed lower jaw which is held to the base, where the other end of the test material is clamped. When the material is safely held by the two jaws, the command is given from the computer connected to

the machine, to start the test. This initiates the steady elongation of the material by the upward movement of the movable upper jaw. The movement is controlled by the elongation rate of the material, which is also known as the test speed as the elongation rate is dependent on the speed at which the upper jaw rises. The test automatically stops at the point where the material breaks. The schematic diagram of the tensile testing machine can be shown in Figure 8 (on the next page). This initiates the steady elongation of the material by the upward movement of the movable upper jaw. This

initiates the steady elongation of the material by the upward movement of the movable upper jaw.

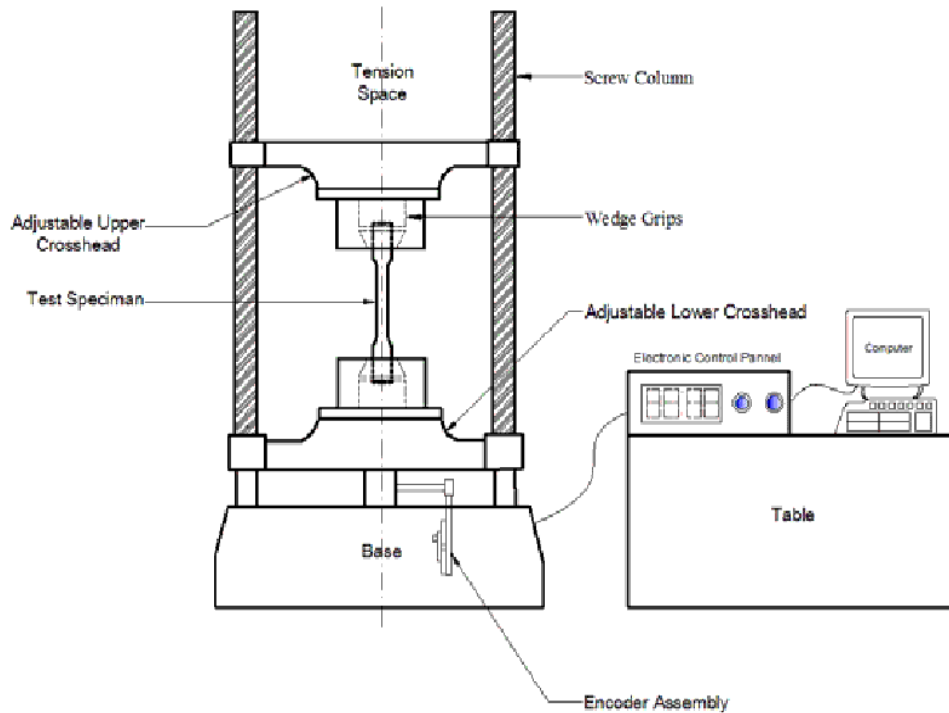


Figure 3.6: Schematic diagram of Tensile Testing Machine [49]

Tensile testing of all the samples i.e. 0.5%, 1%, 1.5%, 2% TiO₂/PA/frmic acid membrane is carried out, using SHIMADZU AGS-X series precision ultimate tensile tester with a full load of 20 KN. All of the samples were tested using the ASTM standard D872- 02, so the strips to be used were cut according to the dimensions provided by the standard. Finally, the stress-strain behavior was studied for the tests conducted using the said standard.

3.4.4: Working Principle of Hollow tubes formation System.

For the formation of hollow tubes 1st time in SCME I arranged a device which is connected with gas cylinder to provide 0.98bars pressure to the solution of 20%w/v polyamide-6 solute(0.5%w/w TiO₂) in polymer solution injection port which is connected with device ,the device having two tubes one is internal tube(Injection port for bore forming fluid)(water,air,oil) which is filled with air or water or oil and external tube(polymer solution injected port) is getting polyamide solution ,the air gap..

coagulation bath for 5 mins to exchange solvent(Formic acid) with water(Washing tank) and keeping it in oven for 35 C⁰(Heat treatment) which are as follows.

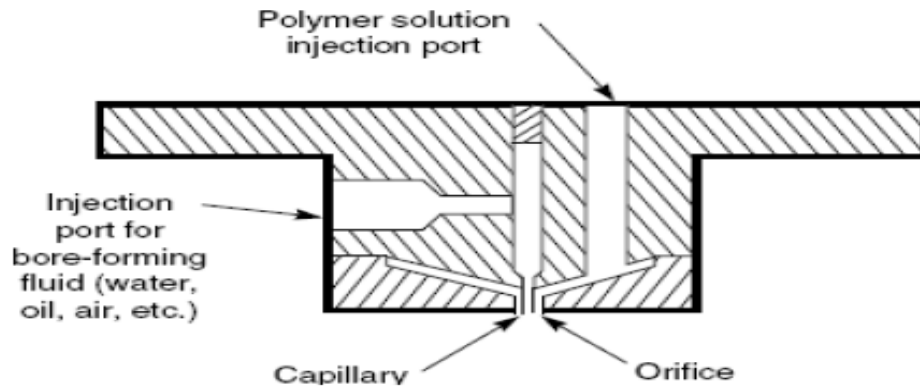


Figure 3.7: Schematic diagram of Hollow fiber formation device [50]

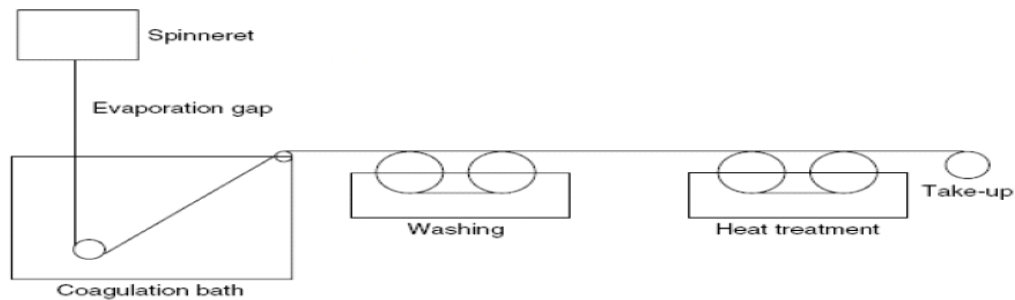


Figure 3.8: Schematic diagram of Hollow fiber formation device [51]

3.4.5: Working Principle of water Flux Testing System

In a water permeation test system, we find out the permeability of the water through the membrane. Permeability is the measure of the ability of a fluid to pass through a porous media. The permeability co-efficient, P , is defined as: Moreover, the permeation of water through the same membrane can be used to find the rejection of salt % of one particular salt over another. The rejection of salt % of salt A over salt B is found by the following equation: For single salt permeation testing, a stainless steel permeation rig is used. The permeation rig is used for testing the permeance of water through a membrane. The membrane is fitted into the membrane cell. Feed water is introduced at the top of the cell while permeate is exited from the bottom of the cell. For the purpose of finding out the flow rate of permeate water, a portion of that salt is taken through a bubble flow meter, in which the time taken for the bubble to flow a

fixed volume gives us the water flow rate. The schematic diagram of the permeation rig is shown in Figure: The below fig shows one is feed tank in which salt water is filled while the other one shows permeate tank in which water is stored after removal of CaCl_2 salt which are connected with pump that suck feed water from feed tank and provided to bottles in which we fixed Poly amide-6 fabricated polymer having 0.5% TiO_2 /FA by doing small pores in it then by providing 101Kpa pressure to it we have observed 97% salt rejection which can be seen in UV testing and $38 \text{ Lm}^2/\text{hr}$ which is matching with literature reading almost.

The permeate water also tested from PH meter showed PH round about 7.4 can be seen.



Figure 3.9 : Schematic diagram of water permeability testing system UV spectroscopy

For the purpose of single water permeability testing, we have used the UV spectroscopy Permeability. Test System which has stainless steel permeation rig in it. The membranes are tested for permeation of water and salts at different gauge pressures, from 60 bar to 73 bars. After doing this testing, permeability of water and salt rejection % are calculated.

3.4.6: Working Principle of UV spectroscopy

UV is an analytical technique, in which a solution of two or more liquids or salt mixture (the test sample) is fed in with a mobile phase, over a stationary phase. The stationary phase may be a solid or a liquid adsorbed on a solid. The distribution of the different components of the feed mixture between the stationary and mobile phases, helps in the separation and analysis of the components of the mixture. Chromatography can be classified on the basis of a number of classifications. One classification is on the basis

of phases used, which includes liquid chromatography and gas chromatography. Gas Chromatography (GC) is a general, broad term used for any type of chromatography, in which gas is used as the mobile phase. It is further divided into gas-solid chromatography (GSC) and gas-liquid chromatography (GLC). For mixed salt water permeation testing, chromatography (GC) is used. The permeate from permeation rig or permeation cell is connected to Chromatograph, for analysis of composition of permeate coming out of the membrane. The composition of permeate gas will determine how much of each salt water mixer passes through the membrane, and hence will give us the salt rejection % of the membrane for either of the salt water. The reactor used for that type of salt water, in which the mobile phase is water [51]. Chromatography is also carried out in an apparatus called Gas Chromatograph. A typical reactor consists of the following pieces of equipment:

- Gas tank providing pressure of 101kpa
- Sample injection port
- GC column
- Detector
- Attenuator
- Chart recorder
- Two pumps
- Feed tank
- Permeate tank

Feed solution (CaCl₂ dissolved water provided to Poly amide-6 membrane.

Moving on, we see a sharp peak at 2865.61 cm⁻¹, signifying the presence of C_{sp}³-H bond. Lastly, we see a peak at 1641.95 cm⁻¹, thereby confirming the presence of C=O bond. Moving on to the next sample, it is seen that, there is an inverted bell-shaped curved peak at a wave number of 3484.71 cm⁻¹ for the membrane containing 0.1% TiO₂.

The composition of permeate gas will determine how much of each salt water mixer passes through the membrane, and hence will give us the salt rejection % of the

membrane for either of the salt water. The reactor used for that type of salt water, in which the mobile phase is water [50]. Chromatography is also carried out in an apparatus called Gas Chromatograph. The composition of permeate gas will determine how much of each salt water mixer passes through the membrane, and hence will give us the salt rejection % of the membrane for either of the salt water. The reactor used for that type of salt water, in which the mobile phase is water [51]. Chromatography is also carried out in an apparatus called Gas Chromatograph. However, if we compare this peak to that of pure PA membrane, it is seen that it is much broader; this indicates the presence of a secondary amine group. Then, there is another peak, due to the stretching vibration of $C_{sp^3}-H$ bond at wave number of 2865.05 cm^{-1} . Another major peak of the spectrum is at a value of 1639.89 cm^{-1} which confirms the presence of a $C=O$ double bond. The rejection of salt % of salt A over salt B is found by the following equation: For single salt permeation testing, a stainless steel permeation rig is used.

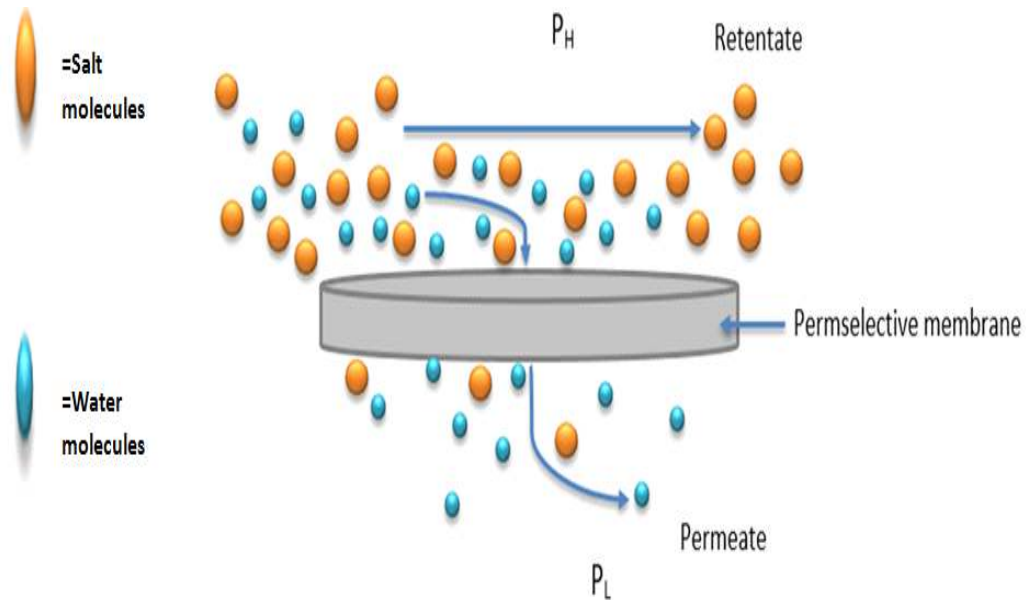


Figure 3.10 : Permeance molecule and retentate molecule

The carrier salt water is fed into the sample injection port, where our test salt water samples are also kept. Both the carrier salt water and the feed water are mixed, and introduced into the reactor column. The column is filled with the stationary phase, which interacts differently with different components of the feed whereas the carrier salt water does not interact with the stationary phase. At the end of the column is detector which measures the amount of each salt water exiting the column. The

column is kept at elevated temperatures, to keep the sample in vapour phase. displayed as a graph called *chromatogram*. The arrangement is represented in Figure. Moreover, as the amount of filler increases, the molecular chains of the polymer become less mobile and more rigid as more filler is added, which would hinder the permeability of water molecules [70].

Moreover, as the amount of filler increases, the molecular chains of the polymer become less mobile and more rigid as more filler is added, which would hinder the permeability of water molecules [71].

Moreover, as the amount of filler increases, the molecular chains of the polymer become less mobile and more rigid as more filler is added, which would hinder the permeability of water molecules [72]. For mixed salt water permeation and separation testing, Perkin-Elmer Clarus 237nm UV graph is used. CaCl₂/H₂O salt mixture is used as the feed salt for this purpose, which passes through the membrane.

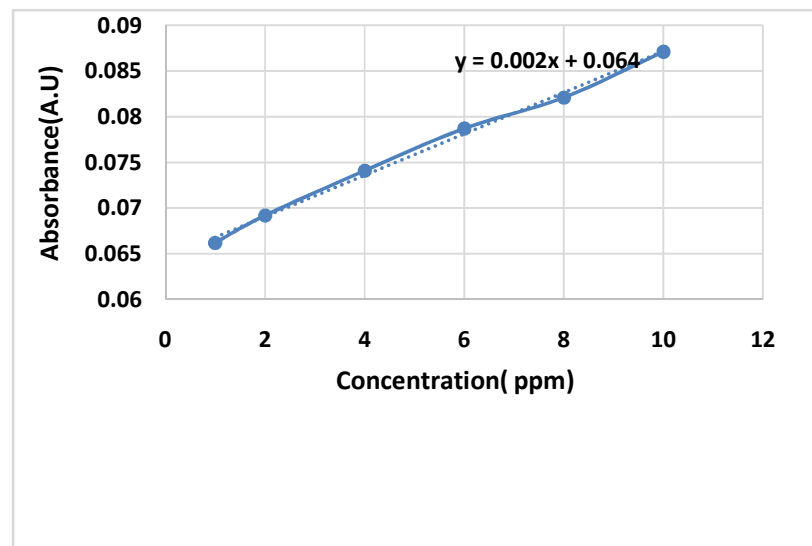


Figure 3.11:Permeance molecule and retentate molecule through UV spectroscopy

Table 3.1: UV spectroscopy results

Concentration (mg/l)	Absorbance
1	0.0562
2	0.0692

4	0.0741
6	0.0887
8	0.0921
10	0.0971

Table 3.2: UV spectroscopy results

	Absorbance	Concentration(mg/l)
Inlet concentration	0.0871	10
Permeation Concentration	0.0652	0.03347826

The feed salt mixture into the column is the flux which has passed through the membrane. The testing is carried out at different pressures, just like in the case of single salt mixture permeation testing which come out in the form of a UV (ultra violet) spectroscopy but this one shows 73% salt rejection which is not satisfaction or match with literature review. The salt rejected through this way is 97.5 % and flux through this way is 40 and 41 Lm²/hr. The above graph shows 73% salt rejection which not enough is because our literature shows that salt rejection % should above than 95% .Through UV graph of calibration. Firstly, we have the spectrum of the membrane sample made of pure Formic acid. It contains a perfectly bell-shaped inverted peak at the wave number value of 3487.71 cm⁻¹, which is due to the stretching vibrations of the N-H bond. Moving on, we see a sharp peak at 2865.61 cm⁻¹, signifying the presence of C_{sp}³-H bond. Lastly, we see a peak at 1641.95 cm⁻¹, thereby confirming the presence of C=O bond. Moving on to the next sample, it is seen that, there is an inverted bell-shaped curved peak at a wave number of 3484.71 cm⁻¹ for the membrane containing 0.1% TiO₂. It is because of stretching vibrations of the N-H bond. However, if we compare this peak to that of pure PA membrane, it is seen that it is much broader; this indicates the presence of a secondary amine group present in the poly amide-6. At this thickness it also shows maximum flux by varying pressure from 90 KPa , 100KPa , 110KPa, 120 KPa, 130 KPa. AT 130KPa Poly amide-6 having filler concentration is 0.5 % show maximum mechanical strength and flux at lower TiO₂ loadings up to 1%. And lastly, we decided to carry out tensile strength testing for polymer blend membranes as well. As a representative, we decided to take one sample. So, we took 2% TiO₂ in PA(Poly amide-6)/FA(Formic acid) membranes. It is

seen that the resulting membrane has far less tensile strength than any of the TiO₂ Powder/PA /FA membranes and even less strength than the PA/FA membrane with no TiO₂ Powder in it. This means that addition of PA has indeed reduced the interfacial bonds between the polymer chains, thus lowering the strength to a value even below that of the neat polymer membrane. Moreover, the addition of TiO₂ Powder can also be explained by the interfacial interactions of filler and polymer. It is seen that the resulting membrane has far less tensile strength than any of the TiO₂ Powder/PA /FA membranes and even less strength than the PA/FA membrane with no TiO₂ Powder in it. This means that addition of PA has indeed reduced the interfacial bonds between the polymer chains, thus lowering the strength to a value even below that of the neat polymer membrane.

. Firstly, we have the spectrum of the membrane sample made of pure Formic acid. It contains a perfectly bell-shaped inverted peak at the wave number value of 3487.71 cm⁻¹, which is due to the stretching vibrations of the N-H bond. Moving on, we see a sharp peak at 2865.61 cm⁻¹, signifying the presence of C_{sp}³-H bond. Lastly, we see a peak at 1641.95 cm⁻¹, thereby confirming the presence of C=O bond. Moving on to the next sample, it is seen that, there is an inverted bell-shaped curved peak at a wave number of 3484.71 cm⁻¹ for the membrane containing 0.1% TiO₂. It is because of stretching vibrations of the N-H bond.

Chapter 4

Results and Discussion

4.1: Characterization techniques

Different characterization techniques have been used to analyze the membranes for their different properties. The various techniques used for characterization are as follows:

- Fourier Transform Infra-Red (FT-IR) Spectroscopy, used to analyze the different functional groups within the poly amid -6 contain different % of fillers membrane structure
- Scanning Electron Microscopy, used to analyze and observe the surface morphology and pore characteristics of the membrane
- Tensile testing analysis, used to test the mechanical strength of the membranes.
- X-rays diffraction (XRD) which is used for presence of fillers in poly amid-6 membrane by showing peaks at above 33 degree.
- X-rays diffraction (XRD) of titanium di oxide (TiO₂) which show many peaks.
- UV testing which give us graph to show salt rejection %.
- Flux of water can be find by using simple method in which we adjusted gas cylinder with the bottle os solution having 0.0037m² area in the cape of bottle in which flate is fixed for finding flux through flow rate and specific time.
- UV testing which give us graph to show salt rejection %.
- Flux of water can be find by using simple method in which we adjusted gas cylinder with the bottle os solution having 0.0037m² area in the cape of bottle in which flate is fixed for finding flux through flow rate and specific time.

4.1.1 (a) : FT-IR Spectroscopy Analysis

Fourier Transform Infra-Red (FT-IR) Spectroscopy, used to analyze the different functional groups within the poly amid -6 contain different % of fillers membrane structure.

. Finally, the stress-strain behavior was studied for the tests conducted using the said standard. The presence of different functional groups is confirmed by analyzing the various membrane samples using FT-IR spectroscopy. Firstly, we have the spectrum of the membrane sample made of pure Formic acid

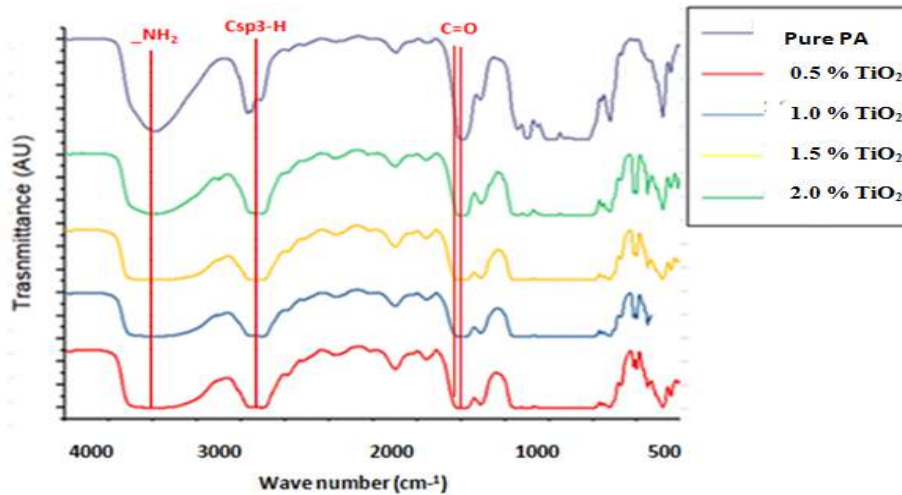


Figure 4.1: FT-IR spectra of (i) Pure PA/FA mixed matrix membranes and TiO₂/PA/FA polymer blend membranes

4.1.1 (b) : FT-IR Spectroscopy Analysis.

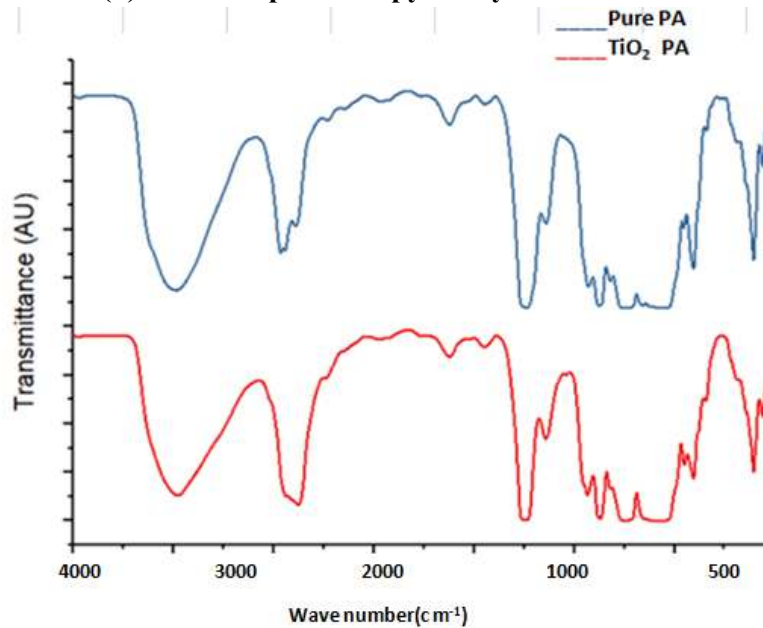


Figure 4.2: FTIR spectroscopy of pure poly amide-6 and % of TiO₂

The presence of different functional groups is confirmed by analyzing the various membrane samples using FT-IR spectroscopy. Firstly, we have the spectrum of the membrane sample made of pure Formic acid. It contains a perfectly bell-shaped inverted peak at the wave number value of 3487.71 cm⁻¹, which is due to the stretching

vibrations of the N-H bond. Moving on, we see a sharp peak at 2865.61 cm^{-1} , signifying the presence of $\text{C}_{\text{sp}^3}\text{-H}$ bond. Lastly, we see a peak at 1641.95 cm^{-1} , thereby confirming the presence of C=O bond. Moving on to the next sample, it is seen that, there is an inverted bell-shaped curved peak at a wave number of 3484.71 cm^{-1} for the membrane containing 0.1% TiO_2 . It is because of stretching vibrations of the N-H bond. However, if we compare this peak to that of pure PA membrane, it is seen that it is much broader; this indicates the presence of a secondary amine group. Then, there is another peak, due to the stretching vibration of $\text{C}_{\text{sp}^3}\text{-H}$ bond at wave number of 2865.05 cm^{-1} . Another major peak of the spectrum is at a value of 1639.89 cm^{-1} which confirms the presence of a C=O double bond. Similarly, for the membrane sample containing 0.5% TiO_2 , we see an inverted bell-shaped peak at 3468.15 cm^{-1} which again signals the presence of an N-H bond, which is present due to the presence of TiO_2 in poly amide-6. Here again, we see that the peak is broader than an ordinary N-H group peak, which is due to the presence of secondary amine group, once again. Moving further, we see a peak at 2888.93 cm^{-1} , which again shows the presence of a $\text{C}_{\text{sp}^3}\text{-H}$ bond due to the C-H backbone of PA. Furthermore, the presence of sharp peak at 1639.86 cm^{-1} due to the presence of C=O bond of the acetate group in PA. Finally, there is a small peak at the left edge of the spectrum, close to 3000 cm^{-1} , which is due to the presence of the N-H bond of a secondary amine group, which shows that amine-modified TiO_2 is indeed present in the structure. In a similar manner, we see the spectrum for 1.5% TiO_2 in PA/Formic acid membrane. The most prominent peak at the very start is the bell-shaped peak at 3485.32 cm^{-1} . This peak is present because of the presence of N-H bond. It is again very broad, which confirms the presence of a secondary amine group. Then, we have a sharp peak at 2878.18 cm^{-1} which is again due to the presence of $\text{C}_{\text{sp}^3}\text{-H}$ bond. Then, we have another sharp peak at 1735.92 cm^{-1} , which confirms the presence of a C=O bond of the acetate group here as well. Finally, we have the spectrum of the sample containing 1.75% TiO_2 in PA/Formic acid membrane. Here, again we see a sharp, inverted bell-shaped peak at 3473.15 cm^{-1} , which can be identified as the N-H bond due to the presence of Formic acid, which is broadened by the presence of a secondary amine group. Then, there is another sharp peak at 2872.18 cm^{-1} , due to the presence of $\text{C}_{\text{sp}^3}\text{-H}$ bond in the carbon-hydrogen backbone. Then, we see another sharp peak at 1735.81 cm^{-1} due to the presence of C=O bond. Then, we move on to the FTIR spectrum of 2% TiO_2 PA/FA blend membranes. Here, we have again included the spectrum of pure PA for comparison.

We see that the spectrum of TiO₂/PA/FA membrane contains an inverted bell-shaped peak at 3470.92 cm⁻¹ which is again due to the presence of N-H bond stretching vibrations and it is very slightly broader than that of pure PA, which again indicates the presence of a secondary amine group. Then, we see the presence of a peak at 2867.17 cm⁻¹ which indicates the presence of C_{sp}³-H bond and the final peak is that at 1734.53 cm⁻¹ which confirms the presence of C=O bond. The most prominent peak at the very start is the bell-shaped peak at 3485.32 cm⁻¹. This peak is present because of the presence of N-H bond. It is again very broad, which confirms the presence of a secondary amine group. Then, we have a sharp peak at 2878.18 cm⁻¹ which is again due to the presence of C_{sp}³-H bond. . Another major peak of the spectrum is at a value of 1639.89 cm⁻¹ which confirms the presence of a C=O double bond. Similarly, for the membrane sample containing 0.5% TiO₂, we see an inverted bell- shaped peak at 3468.15 cm⁻¹ which again signals the presence of an N-H bond, which is present due to the presence of tio₂ in poly amide-6. Similarly when filler is dispersed in the poly amide-6 by different percentage in it.

4.2: Tensile testing.

As shown in Figure 4.3, the ultimate tensile strength of all the membrane samples is measured at an elongation rate of 0.50 mm/min. This value of elongation is picked after several runs with both high and low elongation rates ranging from 0.1 to 1 mm/min. When the elongation rate is too low, the tensile strength is much higher than it should be; whereas if the elongation rate is too high, the tensile strength is much lower than expected. Only, at a moderate value of elongation rate such as 0.5 mm/min, will the membrane strength be more accurately represented. Once the elongation rate is chosen and the experiment is carried out, it can be seen from Figure 4.3, that the tensile strength increases to a very high value on adding small amounts of TiO₂ Powder such 0.5 % and 1% TiO₂ Powder.

When the elongation rate is too low, the tensile strength is much higher than it should be; whereas if the elongation rate is too high, the tensile strength is much lower than expected. Only, at a moderate value of elongation rate such as 0.5 mm/min, will the membrane strength be more accurately represented. we see an inverted bell- shaped peak at 3468.15 cm⁻¹ which again signals the presence of an N-H bond, which is present due to the presence of tio₂ in poly amide-6. Similarly when filler is dispersed in the poly amide-6 by different percentage in it.

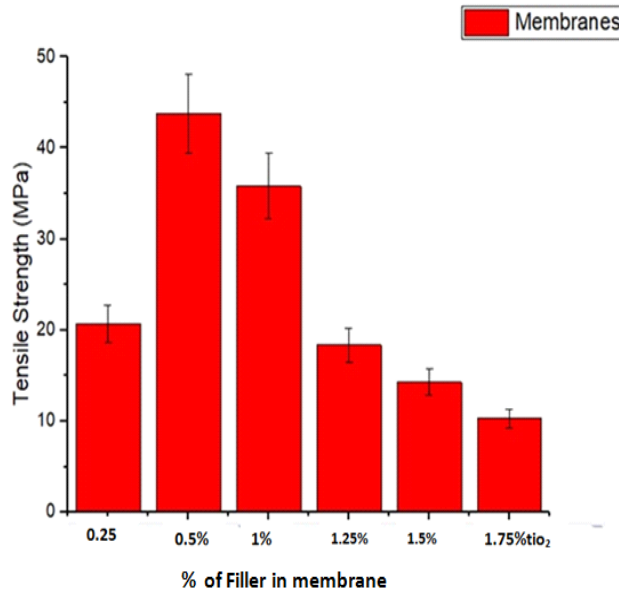


Figure 4.3 (a): Ultimate tensile strength for membrane samples with TiO₂ loading of 0.25%, 0.5%, 1.5%, 1.75% and 2% PA .

However, when the amount of TiO₂ Powder is increased beyond 1%, the value of tensile strength of the membranes drops even lower than that of the membrane with no TiO₂ in its membrane.

This shows that the mechanical properties of membranes are the best at 0.5 % filler in poly amide-6. Once the elongation rate is chosen and the experiment is carried out, it can be seen from Figure 4.4, that the tensile strength increases to a very high value on adding small amounts of TiO₂ Powder such 0.25 % and 1.75 % TiO₂ Powder. This has been explained by Chen et al, and they have stated that the tensile strength of a polymer only decreases with addition of more filler, when the addition of filler causes the interfacial interaction between filler and the neat polymer, to weaken [71]. which can bear pressure up to 130 KPa , 120 KPa , 130KPa.

According to Li et al, the explanation for the decrease in the tensile strength of the mixed matrix membranes (MMMs) on increasing the TiO₂ loading is due to the deteriorating. The reason is that when the area around the filler particles is stiffer than the main polymer phase, then there is less chance of crack formation and propagation. Therefore, as the amount of TiO₂ is increased, the area softens around the filler particle and thus the crack starts to propagate more. This reduces the tensile strength of the membrane on increasing TiO₂ loading, because of increased crack propagation [57]

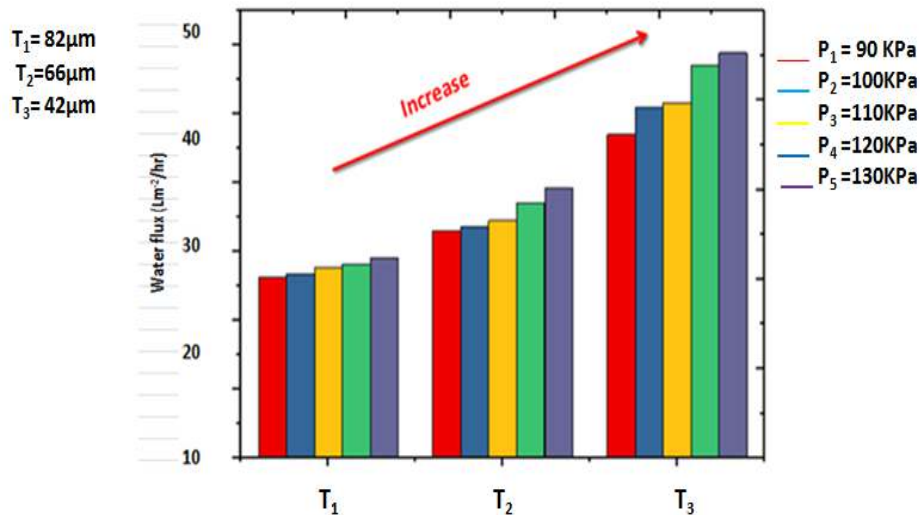


Figure 4.3 (b) Flux and tensile strength which show maximum tensile strength at 42 µm thickness.

This means that addition of PA has indeed reduced the interfacial bonds between the polymer chains, thus lowering the strength to a value even below that of the neat polymer membrane. Moreover, the addition of TiO₂ Powder can also be explained by the interfacial interactions of filler and polymer. According to Li et al, the explanation for the decrease in the tensile strength of the mixed matrix membranes (MMMs) on increasing the TiO₂ loading is due to the deteriorating. The reason is that when the area around the filler particles is stiffer than the main polymer phase, then there is less chance of crack formation and propagation. Therefore, as the amount of TiO₂ is increased, the area softens around the filler particle and thus the crack starts to propagate more. This reduces the tensile strength of the membrane on increasing TiO₂ loading, because of increased crack propagation [57]

.4.4: Scanning Electron Microscopy (SEM) analysis

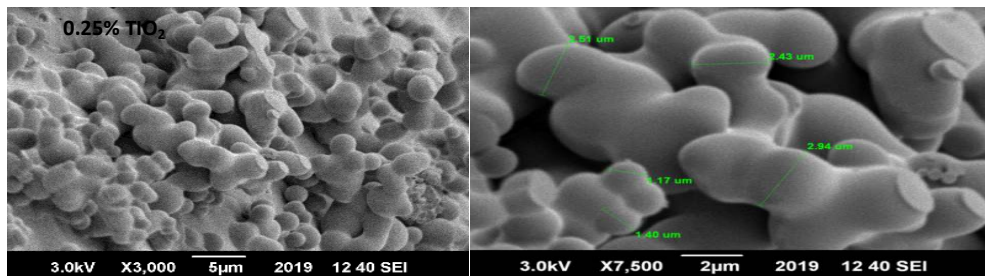


Figure 4.4: SEM images of polymer blend membrane.

This means that addition of PA has indeed reduced the interfacial bonds between the

polymer chains, thus lowering the strength to a value even below that of the neat polymer membrane. Moreover, the addition of TiO_2 Powder can also be explained by the interfacial interactions of filler and polymer. According to Li et al, the explanation for the decrease in the tensile strength of the mixed matrix membranes (MMMs) on increasing the TiO_2 Powder loading is due to the deteriorating stiffness of the polymer/filler interface. The reason is that when the area around the filler particles is stiffer than the main polymer poly amide-6 then it gives us such images of

membrane which are porous in nature, upper porouse size is in nano meters while lower one in microne having mechanical strength of 39.56MPa.

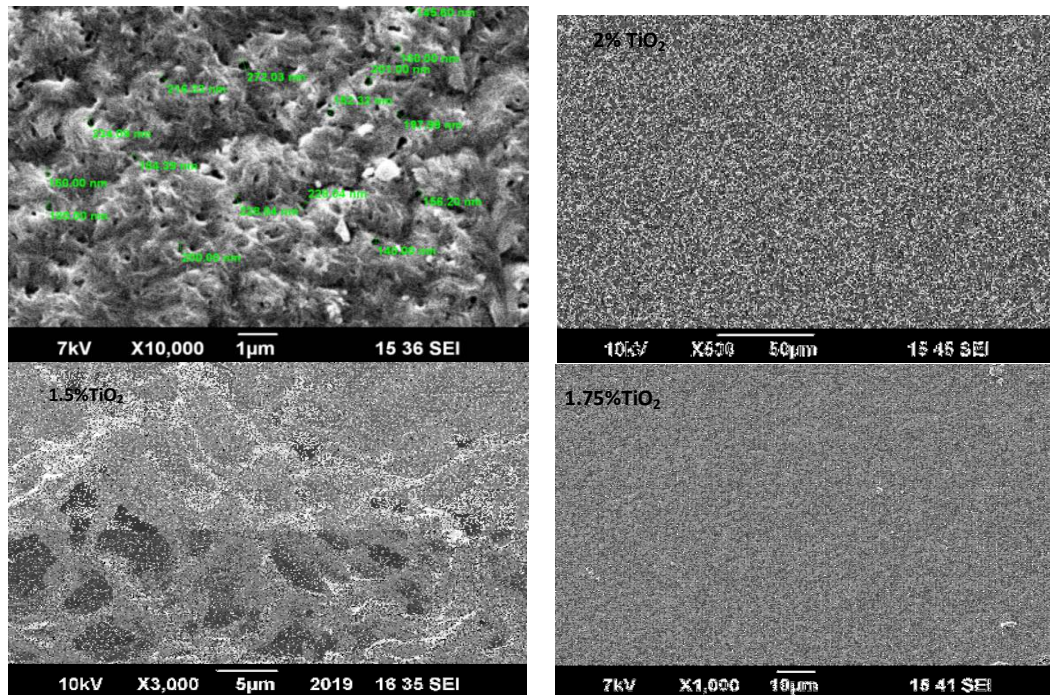


Figure 4.5: SEM images for different % of TiO_2 /

According to Li et al, the explanation for the decrease in the tensile strength of the mixed matrix membranes (MMMs) on increasing the TiO_2 Powder loading is due to the deteriorating stiffness of the polymer/filler interface.

Cross Section Examination

- a) 82 μm Thickness (1.75 TiO_2)
- b) 66 μm Thickness (1.5% TiO_2)
- c) 50 μm Thickness (1.0% TiO_2)
- d) 42 μm Thickness (0.5 TiO_2)

This means that addition of PA has indeed reduced the interfacial bonds between the polymer chains, thus lowering the strength to a value even below that of the neat

polymer membrane. Moreover, the addition of TiO_2 Powder can also be explained by the interfacial interactions of filler and polymer which give us porous membrane with asymmetric membrane having upper pore size is about in nano size while back one size is in micron on 7500 magnification $42 \mu\text{m}$ Thickness (0.5TiO_2).

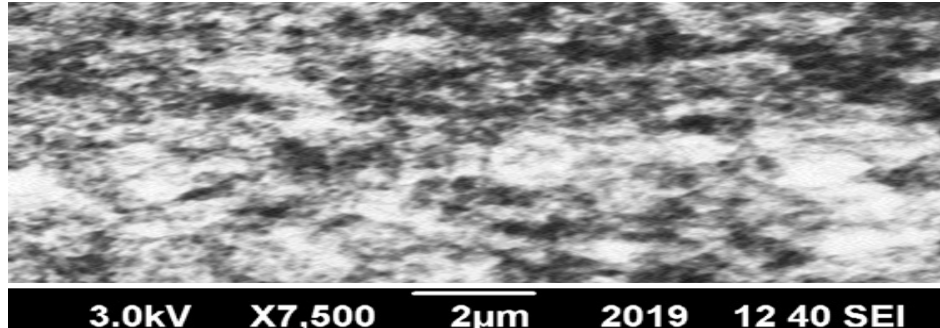


Figure 4.6: SEM images of polymer blend membrane

4.4: Pure Poly amid-6 without Filler.

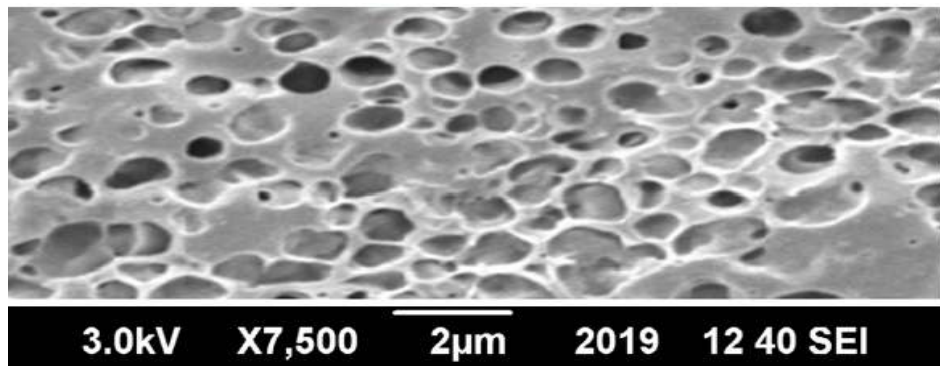


Figure 4.7: SEM Images with different concentration of filler

This means that addition of PA has indeed reduced the interfacial bonds between the polymer chains, thus lowering the strength to a value even below that of the neat polymer membrane. Moreover, the addition of TiO_2 Powder can also be explained by the interfacial interactions of filler and polymer. According to Li et al, the explanation for the decrease in the tensile strength of the mixed matrix membranes (MMMs) on increasing the TiO_2 Powder loading is due to the deteriorating stiffness of the polymer/filler interface. The reason is that when the area around the filler particles is stiffer than the main polymer phase, then there is less chance of crack formation and propagation. Therefore, as the amount of TiO_2 Powder is increased, the area softens around the filler particle and thus the crack starts to propagate more. This reduces the tensile strength of the membrane on increasing TiO_2 Powder loading, because of

membrane on increasing TiO₂ Powder loading, because of increased crack propagation [67].

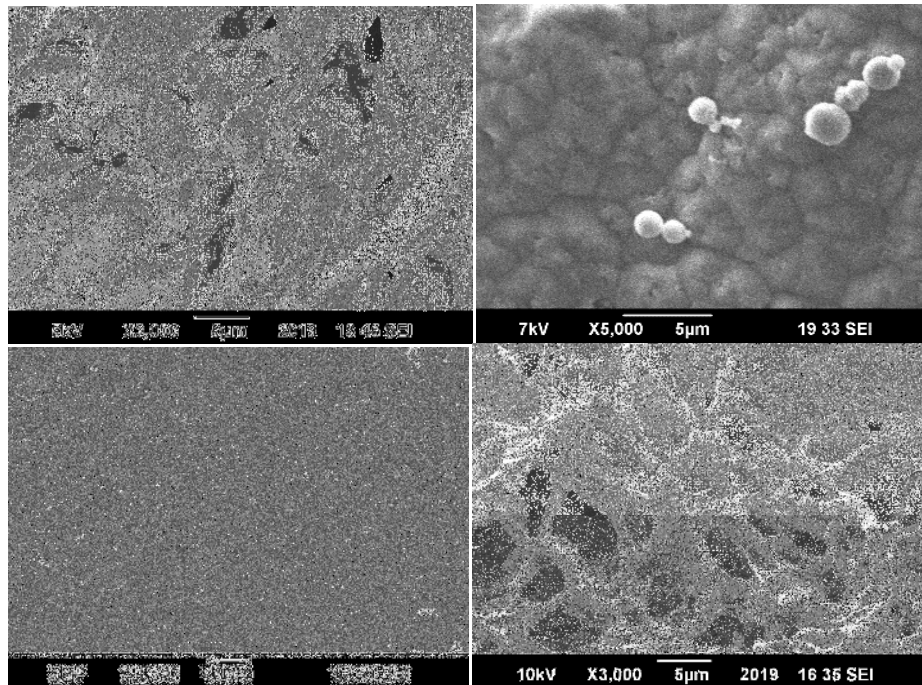


Figure 4.8: SEM Images with different concentration of fillers.

SEM analyses are carried out after the membranes are tested for water permeation properties. Next, we studied the SEM analysis of PA/FA polymer blend membranes. In this analysis, we first study the morphology and surface characteristics of pure PA membranes. In the case of pure PA, for above two images and lower two images for cross sectional of sem images which are different concentration of filler ,these all images are asymmetric in nature upper pores are in nano size and lower one in micron. Also, tracks can be seen in the polymer structure, which is due to the effect of permeation testing on the membranes, as SEM analyses are carried out after the membranes are tested for water permeation properties. Next, we studied the SEM analysis of PA/FA polymer blend membranes. In this analysis, we first study the morphology and surface characteristics of pure PA membranes. In the case of pure PA, Moreover, as the amount of filler increases, the molecular chains of the polymer become less mobile and more rigid as more filler is added, which would hinder .The below SEM images are also cross sectional of membrane which are having different filler % but all of them are porous and asymmetric in nature give good result.In both case of flux and salt rejection % which was 38.5 Lm²/hr flux and 97.5 % retentation.

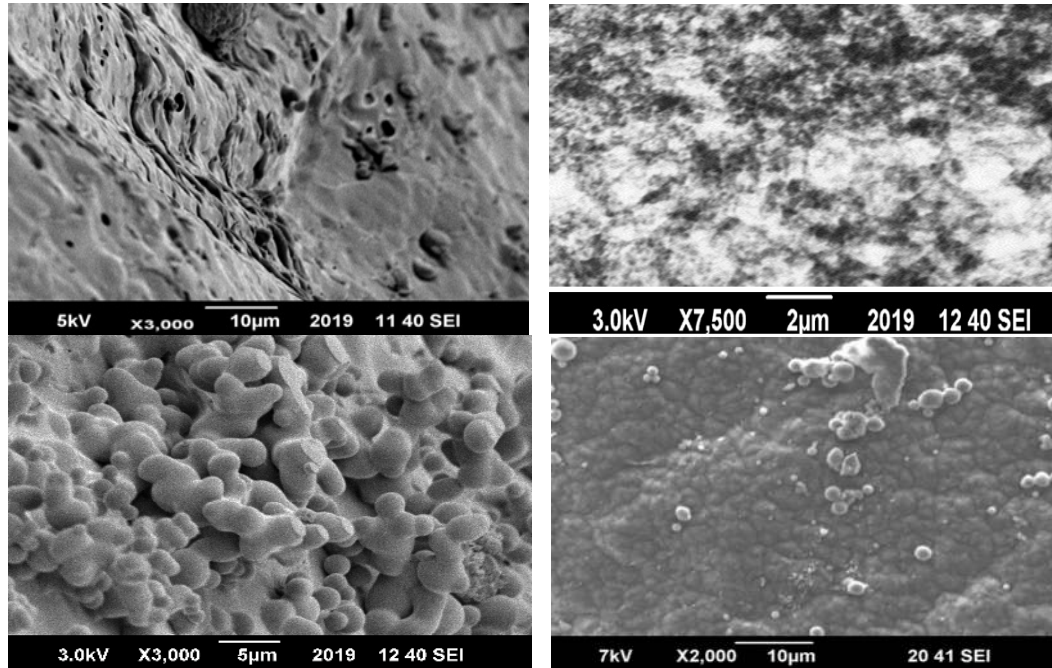


Figure 4.9: Different images of SEM (Scanning electron microscopy) porous polymer.

As shown in Figure 4.6, the different membrane samples were tested using Scanning Electron Microscopy (SEM) analysis. All the samples were analyzed at magnifications of 5000x, 10000x, 15000x, 20000x, 25000x and 30000x. All these samples showed perfectly porous (Asymmetric structures, with white spots dispersed throughout the surface which showed the presence of TiO_2 filler particles. These respective analysis showed that increasing the amount of TiO_2 does greatly affect the pores structure and morphology of the membranes, the spread of the white spots shows the proper dispersion of the TiO_2 in the membrane which gives the membranes their superior salt separation. performance (TiO_2 can repel salt such as CaCl_2).

we observe defect-free and porous surface visible even at high magnifications. As we add TiO_2 in poly amide-6, it can be seen that pores start to appear within the membranes, even at 0.25% w/w. When the amount of TiO_2 in PA is increased even further to about 2% w/w, inter-connected pores are distinctly visible as is seen by the images above. This can be explained by the formation of nano-gaps in the polymer chain on adding larger amounts of TiO_2 in poly amide (PA), as the polymer chains could not properly pack with each other at these high loadings of PA(poly amide-6) .

4.4(i): XRD Characterization

XRD is used for presence of inorganic particles (TiO_2) in poly amide-6 by using formic acid as solvent which show peak at 45 cm^{-1} all three peaks which are matching with each other 1st peak is for pure poly amide-6, second peak is which is having titanium di oxide in poly amide-6 also show same peak, similarly 3rd peak which is composite membrane peak made up of ZIF (zeolite imiodozolate frame work) and poly amid-6 in formic acid also show same peak which is matching with 1st and 2nd peaks in XRD. In the same way curve can also observe for membrane having TiO_2 0.5%,1%,1.5% and 2% also[78]. XRD of titanium di oxide is done which show different peaks,the 1st peak is between 20 and 30 degree similarly the second peak is showing at 39 degree, then at 49 degree it also show peak, while one peak also form at 55 degree, at 64 degree it also shows peaks, double peaks also show at 70 degree, then the last peak is showing it on 75 degree also. In the same pure polymer and filler in the polymeric membrane also show peaks at 34 degree.

TiO_2 is crystalline in nature therefore its showing sharps peaks the 1st sharp peak which is between 20 and 30 degree, while poly amide -6 is amorphous in nature therefore its peaks are not that much sharp same like TiO_2 but when small quantity of filler mix with poly amide-6 its peaks become sharper because Poly amide -6 amorphous nature change into crystalline nature that is why red peaks sharper than blue one which is of pure poly amide -6.

4.4(i): XRD of TiO_2 Characterization

XRD of TiO_2 is sharp comparatively than imporphouse membrane because of crystalline nature of TiO_2 than poly amide-6, In crystalline nature molecules are fixed at their specific position can't change same like imporphouse nature of amide-6

which can't retained salt molecules than titanium di oxide because of retaintation of salt molecule specially of CaCl_2 which can rejected through this filler by 97.5 % and flux $38.5 \text{ lm}^{-2}/\text{hr}$.

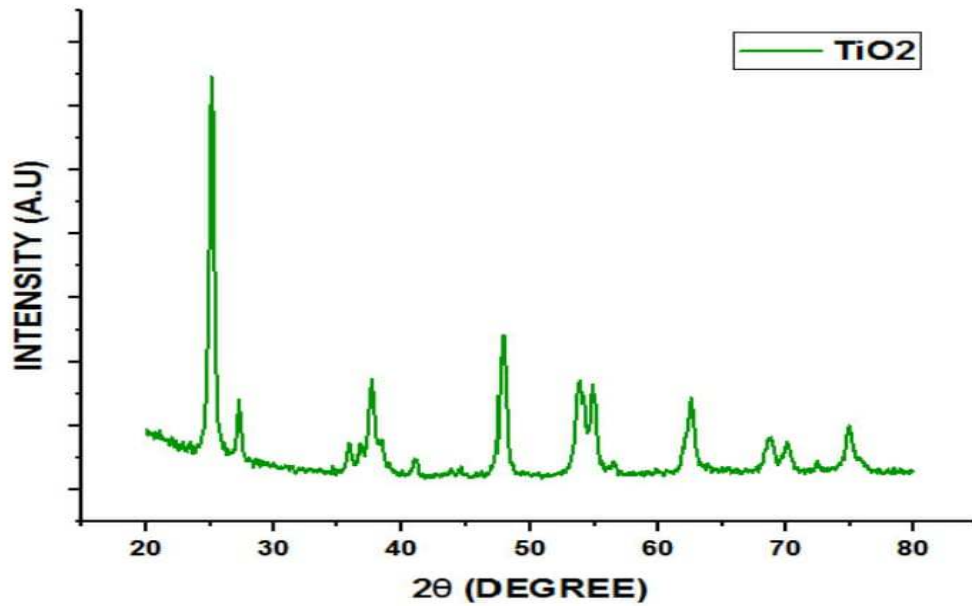


Figure 4.10: XRD images of polymer blend membranes

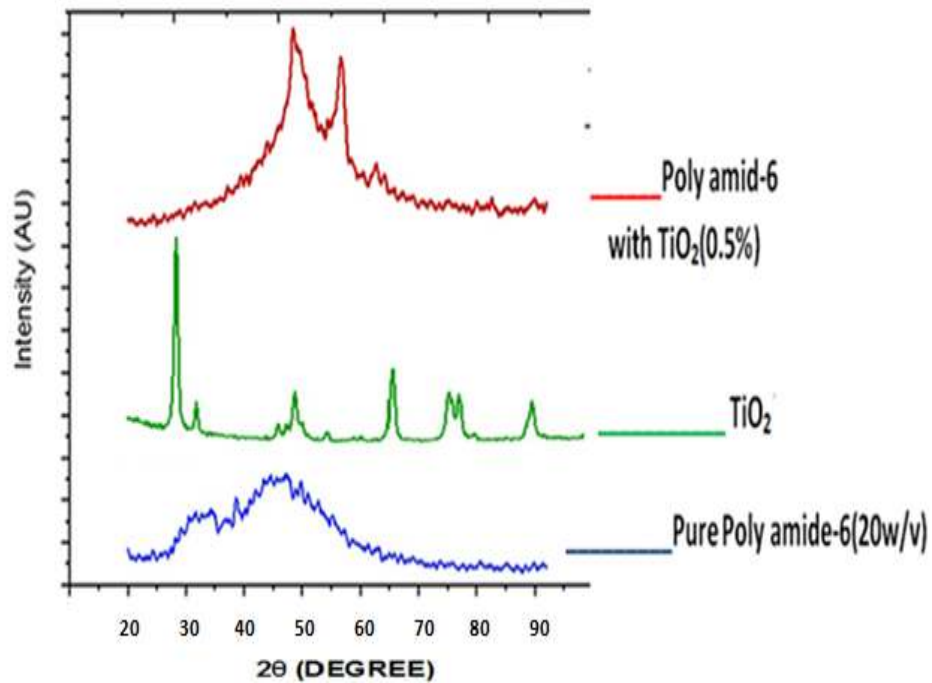


Figure 4.11: XRD images of polymer blend membranes

4.5: Water Flux and salt rejection% Testing.

4.5.1: For polymer blend membranes

Single salt contain water permeation testing was carried out for all the polymer blend membranes containing 0.25%, 0.5%, 1% and 1.5% TiO₂ in PA/FA membranes. The permeation testing was carried out in the UV Testing System fitted with a. The flux of H₂O through the membranes were calculated at pressure values of 52, 63 and 74 KPa respectively, and corresponding salt rejected % were also calculated, as shown in Table 8 and Table 9 respectively and illustrated graphically in Figure 4.9. The permeability and selectivity values

for 1% and 1.5% TiO₂/ -in-PA/FA membranes is not shown, as these two membranes are porous, and these calculations are not possible.

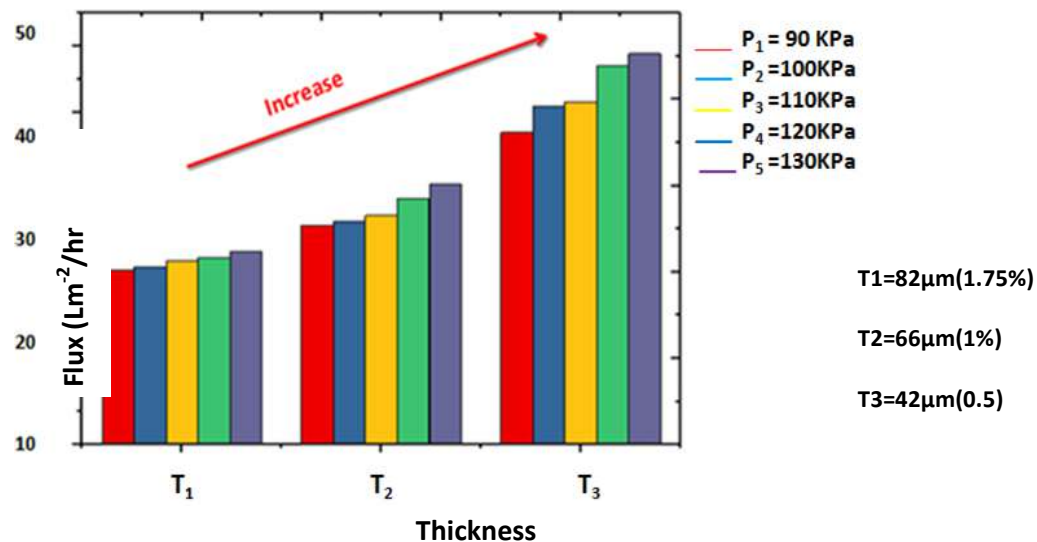


Figure 4.12: show maximum flux at 42μm(0.5%TiO₂) thickness .

Different thickness specially 82μm 66 μm ,50 μm and 42 μm thick membrane strength with flux ratio of 27 Lm⁻²/hr to 40 Lm⁻²/hr respectively and salt rejection % was also between 100% to 90% that was 93% salt rejection and also costly too because of more concentration of filler used in case of filler concentration other than Moreover, as the amount of filler increases, the molecular chains of the polymer become less mobile and more rigid as more filler is added, which would hinder the permeability of water molecules . For water flux and salt rejection % calculation we used different concentration of titanium di oxide which 0.25% ,0.5%, 1%,1.5% and 2% but at 0.5% TiO₂w/w give us 42μm thick layer of poly amide-6 membrane which give us 38Lm⁻²/hr flux. which is matching with literature by using different salt solution (CaCl₂) of 0.25mg/L, 0.5mg/L, 0.75mg/L, 1.0mg/L, 2mg/L, 4mg/L, 6mg/L, 8mg/L

and 10 mg/L give us calibration curve and curve between absorbance and concentration can give us salt rejection % 97.5% while Flux $38.6\text{Lm}^{-2}/\text{hr}$ by using condition of pressure 90kPa to 130KPa the following formula $\text{Flux} = Q(\text{flowrate})/A(\text{Area})$, $\text{Flowrate}(Q) = \text{Flow}/\text{Time}(0.5\text{mL}/35\text{mint}) = (0.01428 \times 57143\text{L}/\text{hr})$ and area in meter is 0.0037m^2 which give us $\text{Flux} = Q(\text{flow rate})/A(\text{Area}) = 38.6\text{Lm}^{-2}/\text{hr}$. Other thickness such as us $82\mu\text{m}$, $66\mu\text{m}$ and $50\mu\text{m}$ was tested for flux and salt rejection % but there result was not that much satisfactory as $42\mu\text{m}$ (0.5% TiO_2) thick membrane which was showing excellent result.

Table 4.1: Flux and salt rejection % of CaCl_2

Concentration of sample	Absorbance
0.1	0.00254
0.25	0.00587
0.5	0.0169
0.75	0.0214
1	0.0428
2	0.0549
4	0.0695
6	0.0761
8	0.0821
10	0.1003

According to Li et al, the explanation for the decrease in the tensile strength of the

mixed matrix membranes (MMMs) on increasing the TiO₂ Powder loading is due to the deteriorating stiffness of the polymer/filler interface. The testing is carried out at different pressures, just like in the case of single salt mixture permeation testing which come out in the form of a UV (ultra violet) spectroscopy but this one shows 73% salt rejection which is not satisfaction or match with literature review. According to Li et al, the explanation for the decrease in the tensile strength of the mixed matrix membranes (MMMs) on increasing the TiO₂ Powder loading is due to the deteriorating stiffness of the polymer/filler interface. The testing is carried out at different pressures, just like in the case of single salt mixture permeation testing which come out in the form of a UV (ultra violet) spectroscopy but this one shows 73% salt rejection which is not satisfaction or match with literature review.

The above results of salts which show excellent results can be seen when before I used filler in smaller quantity or larger quantities that was 0.25=97.5% while before was very less % of salt rejection when flat sheet membrane was coated with filler ratio of 20% w/v of poly amide-6 and keeping filler concentration of 0.25%, 1.0%, 1.5%, 1.75% and 2% it was giving polymeric membrane having thickness of 82 μm, 66 μm, 50 μm, 42 μm, which was showing mechanical strength of 17 MPa, 19 MPa, 28 MPa respectively, only good mechanical strength was showing by membrane was having filler % of 0.5 % w/w having 20% w/v of polymer that mechanical strength was 39.56 MPa which is much better than other which is optimize, that % of filler membrane is giving us 42 μm thick membrane which show good flux with salt rejection % also much better than others as well. Which was having filler ratio of 1.75% of show 19.65 MPa mechanical strength. The 1.75 % of filler having thickness of 82 μm give us flux of 29 Lm⁻²/hr with mechanical strength of 19.65 MPa and salt rejection % is 73% which are as follows. graphs below Which show that when initial concentration was 10 ppm and final concentration was 0.25 ppm which show 97.5 % salt rejection which is we get at optimize condition of filler that was 0.5 % TiO₂ at this % of filler also get excellent mechanical strength that is 39.56 MPa which can bear of pressure from 90 KPa to 130 KPa even loading is due to the deteriorating stiffness of the polymer/filler interface. According to Li et al, the explanation for the decrease in the tensile strength of the mixed matrix membranes (MMMs) on increasing the TiO₂ Powder loading is due to the deteriorating stiffness of the polymer/filler interface. The testing is carried out at different pressures, just like in the case of single salt mixture.

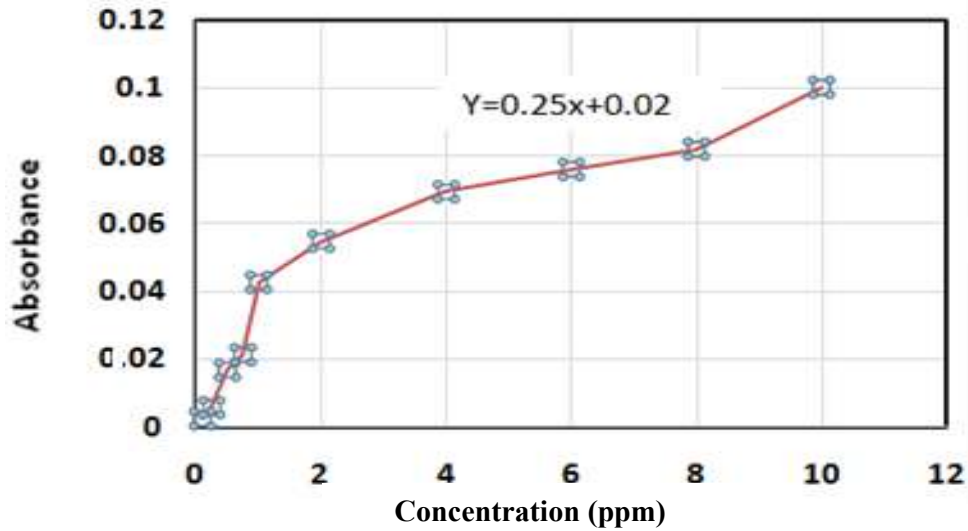
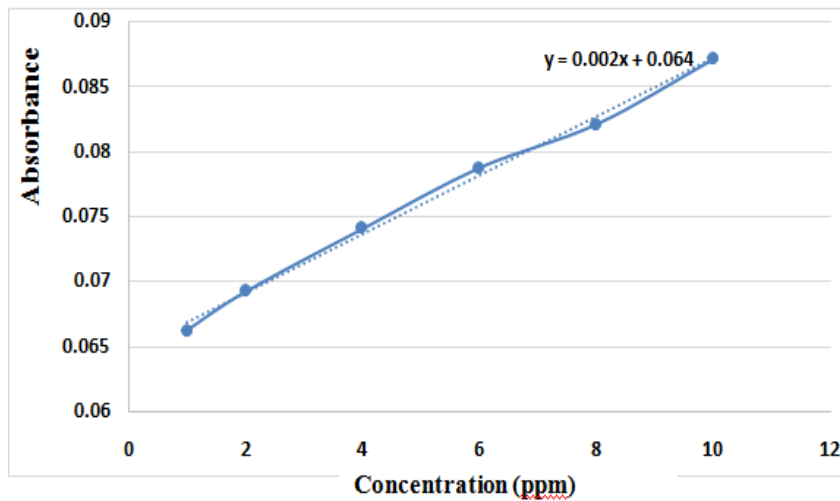


Figure 4.13: UV images of polymer blend membranes



4.14: UV images of polymer blend membranes

According to Li et al, the explanation for the decrease in the tensile strength of the mixed matrix membranes (MMMs) on increasing the TiO₂ Powder loading is due to the deteriorating stiffness of the polymer/filler interface. The testing is carried out at different pressures, just like in the case of single salt mixture permeation testing which come out in the form of a UV (ultra violet) spectroscopy but this one shows 73% salt rejection which is not satisfaction or match with literature review. The salt rejected through this way is 97.5 % and flux through this way is 40 and 41 Lm²/hr. The above graph shows 73% salt rejection which not enough is because our literature shows that salt rejection % should above than 95% .Through UV graph of calibration. Firstly, we

have the spectrum of the membrane sample made of pure Formic acid. It contains a perfectly bell-shaped inverted peak at the wave number value of 3487.71 cm^{-1} , which is due to the stretching vibrations of the N-H bond. in Table 10 below. 0.5 % such that 1.75 % 2 % ,3 % , and polymers comparative than others which are 0.5 % of filler giving us excellent result. According to Li et al, the explanation for the decrease in the tensile strength of the mixed matrix membranes (MMMs) on increasing the TiO_2 Powder loading is due to the deteriorating stiffness of the polymer/filler interface. According to Li et al, the explanation for the decrease in the tensile strength of the mixed matrix

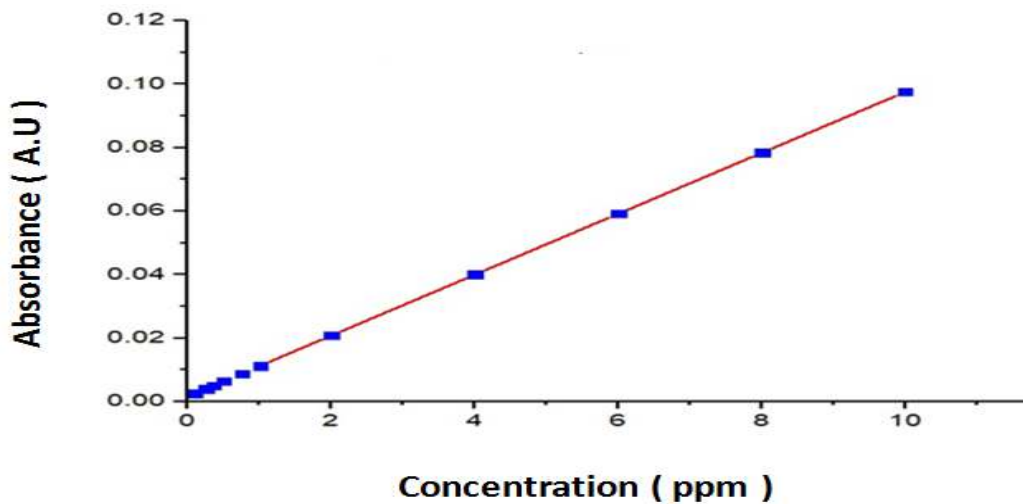


Figure 4.15: UV images of calibration curve for polymer blend membrane

From above all graphs it was proved that only good mechanical strength was showing by membrane was having filler % of 0.5 % w/w having 20% w/v to 22 % w/v of polymer that mechanical strength was 40.00MPa which is much better than other which is optimize , that % of filler membrane is giving us 42 μm thick membrane which show good flux with salt rejection % also much better than others as well . Which was having filler ratio of 1.75% of show 18.65 MPa mechanical strength? The 2.05 % of filler having thickness of 82 μm give us flux of $30 \text{ Lm}^{-2}/\text{hr}$ with mechanical strength of 19.65 MPa and salt rejection % is 73% which are as follows. According to Li et al, the explanation for the decrease in the tensile strength of the mixed matrix membranes (MMMs) on increasing the TiO_2 Powder loading is due to the deteriorating stiffness of the polymer/filler interface. According to Li et al, the explanation for the decrease in the tensile strength of the mixed matrix membranes (MMMs) on increasing the TiO_2 Powder loading is due to the deteriorating stiffness of

the polymer/filler interface. From literature we have studied different polymers with different filler % which vary and also effect on % of flux and salt rejection % which can be seen in the below table of flux and salt rejection % ,which show that when we increases the % of filler it give us minimum flux bt at specific optimize condition it give us maximum flux at 0.5 % filler % at this point it give us maximum salt rejection % which is 97.5 % .

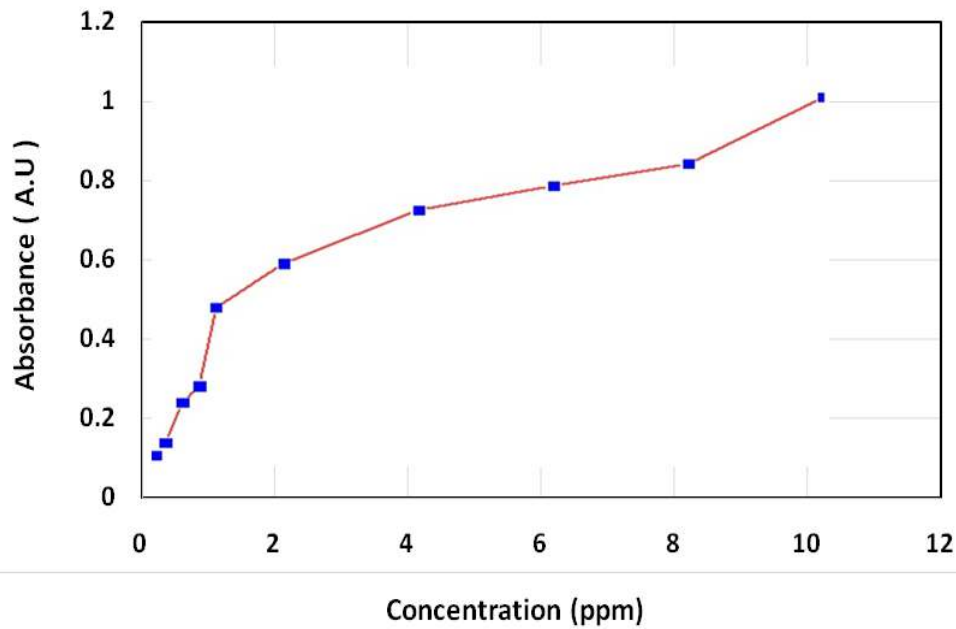


Figure 4.16: UV images of maximum salt rejection% of CaCl₂

Table 9 and Figure 4.12, the salt rejection % of the TiO₂ /PA/FA decreases for CaCl₂/H₂O salt water mixtures, as the amount of PA increases. This is because the CaCl₂ permeation rate decreases as stated earlier, because of the tortuous path that the water molecules have to take, to travel through the membrane, as stated in [70]. This can be explained by the fact that there may be a more tortuous path for the water molecules to travel to get to the permeate side, as the filler is increased.. Where: 55
 seen from Table 9 and Figure 4.12, the salt rejection % of the TiO₂ /PA/FA decreases for CaCl₂/H₂O salt water mixtures, as the amount of PA increases. This is because the CaCl₂ permeation rate decreases as stated earlier, because of the tortuous path that the water molecules have to take, to travel through the membrane, as stated in [72]. This can be explained by the fact that there may be a more tortuous path for the water molecules to travel to get to the permeate side, as the filler is increased. Moreover, as the amount of filler increases, the molecular chains of the polymer become less mobile

and more rigid as more filler is added, which would hinder the permeability of water molecules [72].

Moreover, as the amount of filler increases, the molecular chains of the polymer become less mobile and more rigid as more filler is added, which would hinder the permeability of water molecules [71]. This is because the CaCl_2 permeation rate decreases as stated earlier, because of the tortuous path that the water molecules. According to Li et al, the explanation for the decrease in the tensile strength of the mixed matrix membranes (MMMs) on increasing the TiO_2 Powder loading is due to the deteriorating stiffness of the polymer/filler. As shown in Table 8 above, the permeability decreases, as the amount of TiO_2 in PA/Formic Acid increases. This can be explained by the fact that there may be a more tortuous path for the water molecules to travel to get to the permeate side, as the filler is increased. Moreover, as the amount of filler increases, the molecular chains of the polymer become less mobile and more rigid as more filler is added, which would hinder the permeability of water molecule.

4.3.5: Salt mixture water testing of both flux and salt Rejection %.

The Poly amid-6 membranes containing 0.25%, 0.5%, 1% and 1.5% TiO_2 Powder in PA/Formic Acid membrane, are tested for the permeation of single salt using the stainless steel salt water permeation rig, at subsequent pressures of 51,62,73 and 84 Kpa respectively. The permeation results can be summarized membranes (MMMs) on increasing the TiO_2 Powder loading is due to the deteriorating stiffness of the polymer/filler interface. of the mixed matrix membranes (MMMs) on increasing the TiO_2 Powder loading is due to the deteriorating stiffness of the polymer/filler interface.

According to Li et al, the explanation for the decrease in the tensile strength of the mixed matrix membranes (MMMs) on increasing the TiO_2 Powder loading is due to the deteriorating stiffness of the polymer/filler interface , According to Li et al, the explanation for the decrease in the tensile strength of the mixed matrix membranes (MMMs) on increasing the TiO_2 Powder loading is due to the deteriorating stiffness of the polymer/filler interface. According to Li et al, the explanation for the decrease in the tensile strength of the mixed matrix membranes (MMMs) on increasing the TiO_2 Powder loading is due to the deteriorating stiffness of the polymer/filler interface.

Table 4.3: Membrane type ,Flux and salt rejection %

Membrane type	Flux (Lm⁻²/hr)	Salt Rejection %
Poly amide-6(1.75%)	29	73
Poly amide-6(1.5%)	32	88
Poly amide-6(1.0%)	33	90
Poly amide-6(0.5%)	38.5	97.5
Poly amide-6(2.0%)	37.8	92.5
Poly imide-6(1.75%)	28	90
Poly imide-6(1.5%)	22	80
Poly imide-6(1.0%)	20	85
Poly imide-6(0.5%)	30	66.5
Poly solphoned(1.75%)	31	72
Poly ether sol phone(1.5%)	27	86.5
Poly amide (1.75%)	25	92
PDF (1.5%)	22	76
PDF(1 %)	23	90
PSF	31.5	92.6

This can be explained by the phenomenon of membrane compression on increasing gas pressure [73]. Whereas, increasing the ZIF loading does not have any appreciable effect on the permeability of water molecules. This means that the pore structure of the membrane samples is not altered by increasing ZIF loading. This is proven by the SEM images as shown earlier. The membrane containing 0.1% TiO₂. Moreover, as the amount of filler increases, the molecular chains of the polymer become less mobile and more rigid as more filler is added, which would hinder the flux of water [72].

Table 4.4: CaCl₂ and H₂O permeability and single salt rejections of different concentration of TiO₂/PA membrane

Membrane Type	Filler concentration	Flux (l m ⁻² /hr)	Salt rejection % of CaCl ₂
Poly amide-6	0.25	30	91
Poly amide-6	0.75	32	92
Poly amide-6	0.5	38.5	97.5
Poly amide-6	1.00	35	93.5
Poly amide-6	1.25	36.5	94.5
Poly amide-6	1.50	37	98.5

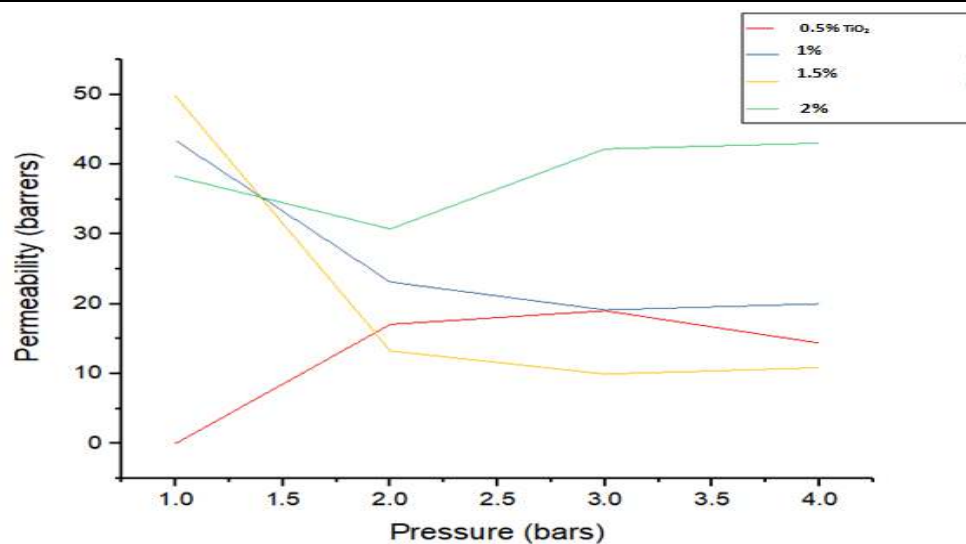


Figure 4.17: Permeability of water in TiO₂/PA membranes at vary pressure

Whereas, as seen from Table 9 and Figure 4.12, the salt rejection % of the TiO₂/PA/FA decreases for CaCl₂/H₂O salt water mixtures, as the amount of PA increases. This is because the CaCl₂ permeation rate decreases as stated earlier, because of the tortuous path that the water molecules have to take, to travel through the membrane, as stated in [72]

Table 4.5: Different salt rejection % of different polymers.

Different salts	ZIF Loaded matrix membranes	Polymer blend membranes
Mixed Salt rejection %	90.49	97.7
CaCl ₂ salt (KPa)(Bars)	92.7485	98.045
MgCl ₂ salt	93.5	92
NH ₄ Cl salt	92	93
Mixture of MgCl ₂ , NH ₄ Cl salts	88	93

Table 4.6: Comparison of flux and salt rejection % of both MMMS and PA membrane

Types of salts	(Flux)	MMMS	Polymer blend membranes	(Flux)(Lm ⁻² /h)
Mixed Salt rejection %	33	98.49	97.7	43.5
Mixture of MgCl ₂ , Iodine	40	91.5	90.61	43.5
Mixture of MgCl ₂ , CaCl ₂ salts	42	90.2	94.5	44.5

Mixture of CaCl ₂ , NaCl salts	33	90.2	95.45	46.5
Mixture of MgCl ₂ , NaCl salts	31	88.5	96.25	41.5
Mixture of MgCl ₂ , CaCl ₂ salts	32	87.53	92.36	38.5
MgCl ₂ salt	28	88.34	93.56	39.5

As seen from the table above, the flux of the polymer blend membranes is much more superior as compared the mixed matrix membranes, but the rejection of salt % is far less. As our basic motive is to separate salts, so our first priority is to choose that material which gives better salt rejection %. Therefore, we have only carried out the mixed salt water permeation testing of the TiO₂ based membranes, to further verify that polymer blend which is having specific ratio of filler in it specific 0.5 % of TiO₂ in it to give excellent result in both flux and salt rejection % which can be seen in the above table but one thing is very clear that is optimization , it means maximum flux which is only show at specific filler concentration that is 0.5 % filler concentration.

. Moreover, as the amount of filler increases, the molecular chains of the polymer become less mobile and more rigid as more filler is added, which would hinder the permeability of water molecules [72]. . Moreover, as the amount of filler increases, the molecular chains of the polymer become less mobile and more rigid as more filler is added, which would hinder the permeability of water molecules [73].

Table 4.7: Flux and salt rejection % of both CaCl₂ & MgCl₂

Sample	Pressure (Bars)	CaCl ₂ Rejection %	H ₂ O (Flux)(Lm ² /h)	MgCl ₂ Salt rejection %
0.25 % TiO ₂	51 bars	92.34	37.5	93.21
	62 bars	98.67	42.5	92.98
	73 bars	91.32	44.65	91.09
	64 bars	91.41	39.5	92

0.5% TiO ₂	81 bars	89.056	33.56	94.12
	72 bars	81.324	34.5	90.21
	63 bars	97.532	37.75	91.21
	74 bars	98.431	36.45	92.16
1.25% TiO ₂	91 bars	92.126	44.54	93.87
	62 bars	90.409	46.35	94.85
	63 bars	98.761	42.54	92.65
	54 bars	89.875	46.5	91.98
1.5% TiO ₂	61 bars	91.236	44.5	93.12
	72 bars	95.481	42.5	94.01
3% TiO ₂	83 bars	95.712	46.5	90.12
0.5 % TiO ₂	103 bars	94.56	39.56	92.5

4.7: Mixed salt water flux testing for poly amide-6(66 μm)

mixture coming out of the permeate of the membrane, and this will give us the salt rejection % of the membrane. The values for the water permeability's and the mixed salt rejection % can be shown in the tables and figures below. This is explained by the compression of the membrane under pressure, as described earlier. This is why all flux reduce by increasing pressure. According to Li et al, the explanation for the decrease in the tensile strength of the mixed matrix membranes (MMMs) on increasing the TiO₂ Powder loading is due to the deteriorating stiffness of the polymer/filler interface , According to Li et al, the explanation for the decrease in the tensile strength of the mixed matrix membranes (MMMs) on increasing the TiO₂ Powder loading is due to the deteriorating stiffness of the polymer/filler interface. According to Li et al, the explanation for the decrease in the tensile strength of the mixed matrix membranes (MMMs) on increasing the TiO₂ Powder loading is due to the deteriorating stiffness of the polymer/filler interface.

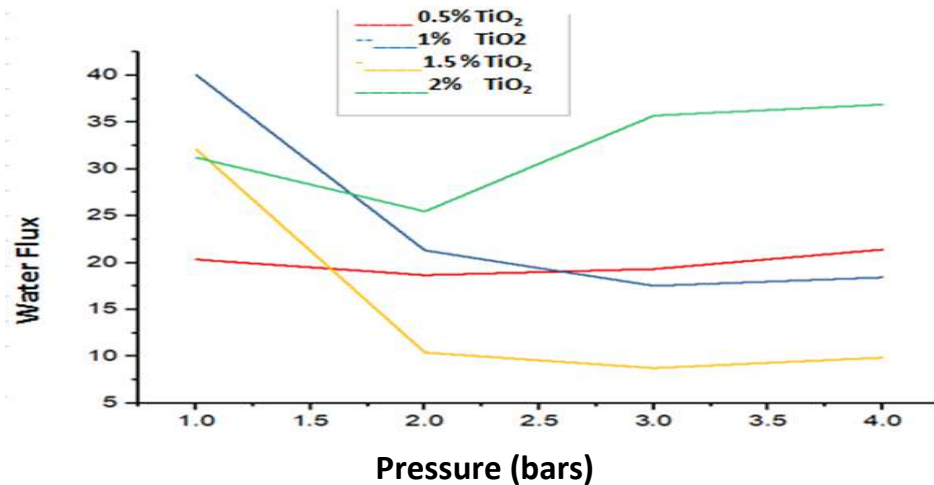


Figure 4.18: water permeability (Flux)(Lm⁻²/h) at vary pressure.

According to Li et al, the explanation for the decrease in the tensile strength of the mixed matrix membranes (MMMs) on increasing the TiO₂ Powder loading is due to the deteriorating stiffness of the polymer/filler interface. According to Li et al, the explanation for the decrease in the tensile strength of the mixed matrix membranes (MMMs) on increasing the TiO₂ Powder loading is due to the deteriorating stiffness of the polymer/filler interface. According to Li et al, explanation for the decrease in the tensile strength of the mixed matrix membranes (MMMs) on increasing the TiO₂ Powder loading is due to the deteriorating stiffness of the polymer/filler interface.

As seen from the table above, the permeability and salt rejection % of the polymer blend membranes is much more superior as compared the mixed matrix membranes, but the rejection of salt % is far less. As our basic motive is to separate gases, so our first priority is to choose that material which gives better salt rejection %. Therefore, we have only carried out the mixed salt water permeation testing of the TiO₂ based membranes, to further verify and consolidate our result can be seen in the above graph .Similarly mechanical strength also not show good one than at that optimize ratio of filler ,at 0.5% filler concentration in the polymeric membrane can show mecha 62 strength of 39.56MPa while other filler concentration ratio below than 20 MI mechanical strength ,Due to filler we also decrease the thickness of membrane from 82μm to 42μm during experiments its noticed ,with the decreasing of thickness it also resist of different fouling such as organic, inorganic ,colloidal , and bio fouling as well ,it also increases the life of membrane as well ,single module can operational up to more than 4 years which is novelty because other module are not perfect same like the above module and also less expensive than others different module of membrane

Conclusions

In this work, two different membranes, the polymer blend membrane containing TiO₂/PA blend in formic acid solvent system, and the mixed matrix membranes containing amino modified TiO₂ as filler in PA continuous phase, were synthesized. The concentrations of fillers and the dispersed polymers were optimized, to observe trends in the permeability and salt rejection %. After the synthesis of the membranes testing of all the various samples was carried out for water permeation, and all the samples were characterized using SEM, FT-IR, XRD, UV spectroscopy and Tensile Testing Analysis. In water flux water testing was carried out for the membranes. FT-IR spectroscopy was carried out to check the availability of the required functional groups ($\text{-NH}_2(3468.5\text{cm}^{-1})$, $\text{CH}_{\text{Sp}3}(2782.5\text{cm}^{-1})$, $\text{C=O}(1720\text{cm}^{-1})$). SEM analysis was done to study the morphology and surface properties of the synthesized membranes which is asymmetric porous membrane. Finally, tensile testing was carried out to check the mechanical integrity of the membrane samples which show maximum elongation at membrane containing 0.5% TiO₂ poly amide-6. It was found through all these testing and characterization techniques, that TiO₂/PA/FA blend membranes are suitable at all, for use as salt separation. The blend membranes give a CaCl₂ maximum salt rejection % of 97.5, whereas the maximum salt rejected obtained from amino-modified PA/FA membrane was 98.49 for single salt testing, and 94.86 for mixed salt testing. Moreover, the tensile strength tests revealed that the maximum tensile strength achieved for PA/FA membranes was 32.56MPa, which is even more than the tensile strength of the unfilled PA/FA membranes. However, the maximum tensile strength obtained from TiO₂ //PA membranes was 39.5673 MPa. Finally, SEM images showed that the TiO₂ /PA membranes were much more porous than the PA/FA membranes, even at high filler loadings (>0.5%). Therefore, it is concluded from this study, that using 0.5% TiO₂ in PA as filler, would yield excellent and unprecedented results, as compared to 2% of TiO₂ in PA/FA membranes. Therefore, it should be made use of in the fabrication of salt separation membranes. Lastly, it is recommended that the blend membranes give maximum salt (MgCl₂) rejection % of 98.5 with 33.63 Lm²/hr, whereas the maximum salt (CaCl₂) rejected obtained from TiO₂ in PA/FA membrane was 97.59 and 94.86 for single salt testing, and mixed salt testing with 38.5Lm²/hr. Moreover, the tensile strength tests revealed that the maximum tensile strength achieved for Poly amide-6 in formic acid with optimize filler concentration.

Future Recommendations

- Further research should be carried out to improve the permeability of the membranes, to make the membranes viable for large scale use.
- Future work should also focus on testing the durability of the membranes for use in harsh conditions
- Automatic caster machine should be used for reducing thickness which enhances performance in both flux and salt rejection %.
- RO is very efficient process for desalination than other conventional techniques due cast, availability and mechanical strength wise also.
- Inorganic particles used in poly amide-6 not only reduces the thickness which enhance performance but also resist different fouling as well such as organic , inorganic, colloidal and biofouling.

Bibliography/References

- [1] F.Y. Liang, M. Ryvak, S. Sayeed, N. Zhao, “The role of water as a primary source in the near future, including comparisons of acquisition, transmission and waste handling costs of as with competitive alternatives”, *Chemical Center Journal*, vol. 2, **2019**, pp. 458-461
- [2] A.B. Wasiu, A. Rashid, A. Aziz, M.R. Heikal, “The Effect of salt Content-water on the Performance Characteristics of health: A Review”, vol. 12, **2012**, pp. 2336-2450
- [3] J. Darmstadter, “Water consumption and Population”, *Resources for the Future*, vol. 4, **2004**, pp. 1-10R. York, “Demographic trends and water consumption in European Union Nations 1960-2025”, *Social Science Resources*, vol. 36, **2007**, pp. 845-872
- [4] N.A. Owen, O.R. Inderwildi, D.A. King, “The status of conventional world water reserves - Hype or cause for concern?”, vol. 39, **2010**, pp. 4733-4739
- [5] R.W. Baker, “Future Directions of Membrane salt Separation Technology”, *Industrial Engineering Chemical Resources*, vol. 41, **2002**, pp. 1383–1401
- [6] A. Douglas, T. Costas, “Separation of salt from Flue Water: A Review”, *Separation Science and Technology*, vol. 40, **2005**, pp. 321-348
- [7] C.H. Yu, C.H. Huang, C.S. Tan, “A review of salt Capture by Absorption” *Journal of Membrane Science*, vol. 135, **1997**, pp. 99-106
- [8] P. Bernardo, E. Drioli, G. Golemme, “Membrane salt Separation: A Review” *RCS Advances*, vol. 18, **2001**, pp. 100-108
- [9] D.R. Paul and Y. R. Yampolskii, “Polymeric Salt Separation Membranes”, 1st ed. Boca Raton, FL: CRC Press, **2000**, *Industrial Engineering Chemical*, vol. 48, **2009**, pp. 4638-4663
- [10] Y.R. Yampolskii and I. Pinnau, “Materials Science of Membranes for salt and Vapour Separation”, 1st ed. Sussex, UK: John Wiley and Sons, **2006**
- [11] T.S. Chung, L. Y. Jiang, Y. Li, and S. Kulprathipanja. “Mixed matrix membranes (MMMs) comprising organic polymers with dispersed inorganic fillers for salt separation”, *Progress in Polymer Science*, vol. 32, **2007**, pp. 483–507.
- [12] P.M. Budd, and N. B. McKeown, “Highly permeable polymers for salt separation membranes”, *Polymer Chemistry*, vol. 1, **2010**, pp. 63–68.

- [13] K.W. Joy, A.J. Willis, W.S. Lacey, "A Rapid Cellulose Peel Technique in Paleobotany", *Annals of Botany*, vol. 20, **1956**, pp. 635-637
- [14] M-W Tang, W.M. King, C.G. Wensley, inventors; Air Products and Chemicals, assignee. Air dried poly amide-6 membranes. United States Patent No. US 4855048; 1989.
- [15] G. Chatterjee, A.A. Houde, S.A. Stern, "Poly(ether urethane) and Poly(ether urethane urea) membrane for CaCl₂/H₂O rejection", *Journal of Membrane Science*, vol. 135, **1997**, pp. 99-106
- [16] M.A. Aroon, A.F. Ismail, T. Matsuura, M.M. Montazer-Rahmati, "Performance studies of mixed matrix membranes(MMS) for salt separation: A review", *Separation and Purification Technology*, vol. 75, **2010**, pp. 229-242
- [17] T.S. Chung, L.Y. Jiang, Y. Li, S. Kalprathipanja, "Mixed-matrix membranes (MMMs) comprising organic polymers with dispersed inorganic fillers for salt separation", *Progress in Polymer Science*, vol. 32, **2007**, pp. 483-507
- [18] P.S. Goh, A.F. Ismail, S.M. Sanip, B.C. Ng, M Aziz, "Recent advances of inorganic fillers in mixed matrix membranes for salt separation", *Separation and Purification Technology*, vol. 81, **2011**, pp. 243-264
- [19] S. Qiu, M. Xue, G. Zhu, "Metal-organic framework membranes: From synthesis to separation application", *Chemical Society Reviews*, vol. 43, **2014**, pp. 6116-6140
- [20] H. Bux, F. Liang, Y. Li, J. Cravillon, M. Wiebcke, J. Caro, "Zeolitic Imidazolate Framework Membrane with Molecular Sieving Properties by Microwave-Assisted Solvo-thermal Synthesis", *Journal of American Chemical Society*, vol. 131, **2009**, pp. 16000-16001
- [21] B. Wang, L.H. Xie, X. Wang, X.M. Liu, J. Li, J.R. Li, "Applications of metal-organic frameworks for green energy and environment: New advances in adsorptive salt separation, storage and removal", *Green Energy and Environment*, vol. 3, 2018, pp. 191-228
- [22] S. Khatua, S. Goswami, S. Biswas, K. Tomar, H.S. Jena, S. Konar, "Stable Multi-responsive Luminescent MOF for Colorimetric Detection of Small Molecules in Selective and Reversible Manner", *Chemical Materials*, vol. 27, 2015, pp. 5349- 5360
- [23] R. Ricco, C Pfeiffer, K. Sumida, C.J. Sumbly, P. Falcaro, S. Furukawa, N.R. Champness, C.J. Doonan, "Emerging applications of metal-organic frameworks", *Crystalline Engineering Communications*, vol. 18, **2016**, pp. 6532-6542

- [24] J.L.C. Rowsell, O.M. Yaghi, “Metal organic frameworks:
- [25] H.C. Zhou, J.R. Long, O.M. Yaghi, “Introduction to Metal Organic Frameworks”, *Chemical Reviews*, vol. 112, **2012**, pp. 673-674
- [26] D. Liu, C. Zhong, “Understanding gas separation in metal-organic frameworks using computer modelling”, *Journal of Materials Chemistry*, vol. 20, **2010**, pp. 45-51.
materials”, *Microporous and Mesoporous Materials*, vol. 73, **2005**, pp. 3-11
- [27] Y. Chen, J. Jiang, “A Bio-Metal-Organic Framework for Highly **rejection %** CaCl₂ Capture: A Molecular Simulation Study”, *Chemicals for Sustainable Chemistry*, vol. 3, **2010**, pp. 982-988
- [28] Y. Li, R.T. Yang, “Salt Adsorption and Storage in Metal Organic Framework MOF-177”, *Langmuir*, vol. 23, **2007**, pp. 12937-12944
- [29] Y. Belmabkhout, A. Sayari, “Effect of pore expansion and amine-functionalization of meso-porous silica on CaCl₂ adsorption over a wide range of conditions”, *Adsorption*, vol. 15 **2009**, pp. 318-328
- [30] T.M. McDonald, W.R. Lee, J.A. Mason, B.M. Wiers, C.S. Hong, J.R. Long, “Capture of Calcium chlorite Flue water in the Amine-Appended Metal-Organic Framework, mmen-Mg₂(dobpdc)”, *Journal of the American Chemical Society*, vol. 132, **2012**, 7056-7065
- [31] X. Wang, H. Li, X.J. Hou, “Amine-functionalized Metal-Organic Membrane As A Highly Selective Adsorbent for CaCl₂ over water”, *Journal of Physical Chemistry C*, vol. 116, **2012**, pp. 19814-19821
- [32] K.S. Park, Z. Ni, A.P. Cote, J.Y. Choi, R. Huang, F.J. Uribe-Romo, H.K. Chae, *Adsorption*, vol. 36, **2007**, pp. 845-872
- M. O’Keeffe, O.M. Yaghi, “Exceptional chemical and thermal stability o zeolitic imidazolate frameworks”, *PNAS*, vol. 103, **2006**, pp.10186-10191
- [33] M. Prakash, N. Sakhavand, R. Shahsavari, “MgCl₂, CaCl₂ and NH₄Cl salt Adsorption in Zeolitic Imidazolate Framework- 95 and -100: Ab Initio Based Grand Canonical Monte Carlo Simulations”, *Journal of Physical Chemistry C*, vol. 117, **2013**, [34] G. Saracco, S. Vankoca, C. Pagliano, B. Bonelli, E. Garrone, “Outer Co (II)

- ions in Co-ZIF-67 salt rejection % adsorb salt from both gas phase and liquid water”, *Physical Chemistry and Chemical Physics*, vol. 16, **2014**, pp. 6139-6145
- [35] N.H. binti-Yahya, Y.S. Yeong, L.S. Lai, “Synthesis of Amino-Impregnated ZIF for urea adsorption” *Adsorption*, vol. 36, **2007**, pp. 845-872
- [36] Z. Zhang, S. Xian, Q. Xia, H. Wang, Z. Li, J. Li, “Enhancement of H₂O on CaCl₂ sal”, *AIChE Journal, Materials*
- [37] B. Seoane, J. Coronas, J. Gascon, “Metal-organic framework based mixed matrix membranes” *Chemical Society Reviews*, vol. 44, **2015**, pp. 2421-2454
- [38] S. Basu, A. Cano-Odena, I.F.J. Vankelecom, “MOF-containing NH₄Cl as mix matrix membrane” *Adsorption*, vol. 38, **2017**, pp. 345-348
- [39] E. Perz, K.J. Balkus Jr., J.P. Ferraris, I.H. Musselman, “Mixed Matrix membrane for urea rejection” *RCS Advance*.
- [40] B. Zornoza, A. Martinez-Joaristi, P. Serra-Crespo, C. Tellez, J. Coronas, J. Gascon, F. Kapteijn, “Functionalized flexible MOFs as fillers in mixed matrix membranes for highly salt rejection % separation of CaCl₂ from H₂O at elevated pressures”, membranes containing MOF-5 for salt separations”, *Journal of Membrane Science, Chemical Communications*, vol. 47, **2011**, pp. 9522-9524
- [41] M.W. Anjum, F. Vermoortele, A.L. Khan, B. Bueken, D.E. de Vos, I.F.J. Vankelecom, “Modulated UiO-66-Based Mixed-Matrix Membranes for CaCl₂ Separation”, *ACS Applied Material Interfaces*, vol. 7, **2015**, pp. 25193-25201
- [42] T. Li, Y. Pan, K.V. Peinemann, Z. Lai, “Carbon dioxide selective mixed matrix composite membrane containing TiO₂ nano-fillers”, *Journal of Membrane Science*, vol. 425, **2013**, pp. 235-242
- [43] H. Bux, C. Chmelik, R. Krishna, J. Caro, “Ethene/ethane separation by the MOF membrane ZIF-8: Molecular correlation of permeation, adsorption, diffusion”, *Journal of Membrane Science*, vol. 369, **2011**, pp. 284-289
- [44] N.A.H.M. Nordin, A.F. Ismail, N. Misdan, N.A.M. Nazri, “Modified ZIF-8 mixed matrix membranes for CaCl₂/NH₄Cl separation”, *AIP Conference Proceedings*, **2017**, 020091

- [45] A. Huang, Q. Liu, N. Wang, J. Caro, “Organo-silica functionalized zeolitic imidazolate framework ZIF-90 membrane for CO₂/CH₄ separation”, *Angewandte Chemie. International Edition*, vol. 51, **2012**, pp. 10551-105
- [46] M.D. McCluskey, “Local Vibrational Modes of Impurities in *Journal of Applied Physics*, vol. 87, **2000**, pp. 3593-3617
- [47] Scanning Electron Microscopy, *Nanoscience Instruments 2018*, Elsevier, Netherlands
- [48] S. Chellamuthu, M.N. Ali, S. Muthu, “Experimental study on tensile behavior of ceramic membranes” *Angewandte Chemie. International Edition*, vol. 51, **2018**, pp.
- [49] A.F. Ismail, W.A. Hafiz, “Effect of poly-sulfone concentration on the performance of membrane-assisted lead acid battery”, *Songklanakarin Journal of Science and Technology*, vol. 24, **2005**, pp.
- [50] R.L. Grob, Introduction in: “Modern Practice of Gas Chromatography”, R.L. Grob, E.F. Barry (eds.), 4th ed., John Wiley and Sons Inc., New Jersey, USA, **2004**, pp. 9-10
- [51] Water Chromatography (Laboratory Manual), What-when-how: In-Depth Tutorials and Information, (Accessed 18th October 2018)
- [52] E.S.S. Mohamed, A. Saleh, A.B. Belal, A.A. Gad, “Application of near-infrared reflectance for quantitative assessment of soil properties”, *Egyptian Journal of Remote Sensing and Space Sciences*, vol. 21, **2017**, pp 54-58
- [53] J.J. Goldstein, D.E. Newbury, J.A. Michael, N.W.M. Ritchie, J.H.J. Scott, D.C. Joy, *Scanning Electron Microscopy and X-Ray Microanalysis*, 4th ed., Springer, New York, **2018**.
- [54] Energy Filtered Transmission Electron Microscopy (EFTEM), Electron Microscopy Center at Indiana University Bloomington, (Accessed 19th October 2019)
- [55] V.G. Rostiashvili, T.A. Vilgis, “Statistical Thermodynamics of Polymeric Materials” *Encyclopaedia of Polymeric Nano-materials*, Springer, Berlin, **2014**.
- [56] H. Li, T. Luo, K. Yang, H.K. Jeong, Y. Dai, G. He, W. Zhao, “Simultaneous enhancement of mechanical properties and CO₂ selectivity of ZIF-8 mixed matrix

membranes: Interfacial toughening effect of ionic liquid”, *Journal of Membrane Science*, vol. 511, **2016**, pp. 130-142

[57] C.J. Holt, J.P. Vizuet, I.H. Musselman, K.J. Balkus Jr., J.P. Ferraris, Polymer Blend Membranes for Gas Separations in: “Membrane for Gas Separations”, M.A. Carreon (ed.), 1st ed., World Scientific, Singapore, **2018**, pp. 195-196

[58] L. Deng, T.J. Kim, M.B. Hagg, “Facilitated transport of CaCl₂ in novel PVAm/PVA membrane” *Journal of Membrane Science*, vol. 135, **1997**, pp. 99-106

[59] D. Wang, K. Li, W.K. Teo, Polyethersulfone hollow fiber salt separation membranes prepared from NMP/alcohol solvent systems, *Journal of Membrane Science*, vol. 115, **1996**, pp. 85-108 of ZIF-8 mixed matrix membranes: Interfacial toughening effect of ionic liquid”, *Journal of Membrane Science*, vol. 511, **2018**, pp. 132-143 , PA blend membrane, *Journal of Membrane Science*, vol. 340, **2009**,

[60] L.G. Toy, B.D. Freeman, R.J. Spontak, Gas Permeability and Phase Morphology *Macromolecules*, vol. 30, **1997**, pp. 4766.

[61] J.W. Barlow and D.R. Paul, Polymer Blends and Alloys: A Review of Selected

[62] N. Panapitiya, S. Wijenayake, D. Nguyen, C. Karunaweera, Y. Huang, K. Balkus Jr., I. Musselman, J. Ferraris, Compatibilized Immiscible Polymer Blends for salt Separations, *Materials*, vol. 9, **2016**, pp. 643-648

[63] L.M. Robeson, Application of Polymer Blends: An Emphasis on Recent Advances, *Polymer Engineering and Science*, vol. 24, **1984**, pp. 587-597

[64] H.A. Mannan, H. Mukhtar, T. Murugesan, R. Nasir, D.F. Mohshim, A. Mushtaq, Recent Applications of Polymer Blends in Salt Separation Membranes, *Chemical Engineering Technology*, vol. 36, **2013**, pp. 1-10

[65] H. Mukhtar, H.A. Mannan, D. Minh, R. Nasir, D.F. Moshshim, T. Murugesan, Polymer blend membrane for CaCl₂ separation from natural water, *IOP Conference Series:Earth and Environmental Science*, vol. 36, no. 1, **2016**

[66] G.C. Kapantaidakis, “ A review on polymeric membranes for salt separation”, *Polymer Engineering and Science*, vol. 21, **1981**, pp. 985-996

[67] S.P. Kaldis, X.S. Dabou, G.P. Sakellariopoulos, Water Permeation though PSf-PI miscible blend membranes, *Journal of Membrane Science*, vol. 110, **1996**, pp. 239-247, Considerations, *Polymer Engineering and Science*, vol. 21, **1981**, pp. 985-996

- [68] Y. Cai, Z. Wang, Z. Yi, Y. Bai, J. Wang, S. Wang, salt and water transport properties of polyallylamine/polyvinyl alcohol/Polysulfone composite membranes, *Journal of Membrane Science*, vol. 310, **2008**, pp. 184-196
- [69] D. Wang, K. Li, W.K. Teo, Polyethersulfone hollow fiber salt separation membranes prepared from NMP/ alcohol solvent systems, *Journal of Membrane Science*, vol. 116, **1996**, pp. 85-108
- [70] J. Li, S. Wang, K. Nagai, T. Nakagawa, A.W.H. Mau, Effect of polyethylene glycol (PEG) on permeabilities and permselectivities in its Poly amide (PA) blend membranes, *Journal of Membrane Science*, vol. 138, **1998**, pp.143-152
- [71] R.S. Chen, S. Ahmed, M.H.A. Ghani and M.M. Salleh, Optimization of high loading on tensile properties of recycled HDPE/PET blends filled with rice husk, *AIP Conference Proceedings*, vol. 46, **2014**
- [72] J.P.G. Villaluenga, M. Khayet, M.A. Lopez-Machado, J.L. Valentin, B. Seoane, J.I. Mengual, salt transport properties of polypropylene/clay composite membranes, *European Polymer Journal*, vol. 43, **2007**, pp. 1132-1143
- [73] K. Klaentschi, J.A. Brown, P.G. Niblett, A.C. Shore, J.E. Tooke, Pressure-permeability relationships in basement membrane: effect of static and dynamic pressures, *American Journal of Physiology*, vol. 274, **1998**, pp. 1327-1334
- [74] D. Bastani, N. Esmacili, M. Asadollahi, "Polymeric mixed matrix membranes containing zeolites as a filler for salt separation applications: A review", *Journal of Industrial and Engineering Chemistry*, vol. 19, **2013**, pp. 375-393
- [75] B. Zornoza, C. Tellez, J. Coronas, J. Gascon, F. Kapteijn, "Metal organic framework based mixed matrix membranes: An increasingly important field of research with a large application potential", *Microporous and Mesoporous Materials membranes for salt separation*, *Separation and Purification Technology*, vol. 16, **2015**, pp. 66-78
- D.Q. Vu, W.J. Koros, S.J. Miller, "Mixed matrix membranes using carbon molecular sieves: I. Preparation and experimental results", vol. 211, **2003**, pp. 311- 334
- [76] H. Cong, M. Radosz, B.F. Towler, Y. Shen, "Polymer-inorganic nano PA as mixed matrix membranes" vol. 14, **2016**, pp. 67-79